From the Department of Neuroscience
Karolinska Institutet, Stockholm, Sweden

ALTERATIONS IN CIRCADIAN ENTRAINMENT – TRANSLATIONAL VALUE IN MAJOR DEPRESSION

Frederik Elberling

Karolinska Institutet

Stockholm 2022

Published by Karolinska Institutet.
Printed by Universitetsservice US-AB, 2022

ISBN 978-91-8016-756-7

Alterations in circadian entrainment – translational value in major depression

THESIS FOR DOCTORAL DEGREE (Ph.D.)

By

Frederik Elberling

The thesis will be defended in public at Petrén Lecture Hall, Nobels väg 12B, Karolinska Institutet, Stockholm, Sweden
Friday, the 30th of September 2022, 09:00

Principal Supervisor:
Prof. Sandra Ceccatelli
Karolinska Institutet
Department of Neuroscience

Co-supervisors:
Dr. Stefan Spulber
Karolinska Institutet
Department of Neuroscience

Prof. Johan Lundberg
Karolinska Institutet
Department of Clinical Neuroscience

Prof. Konstantinos Meletis
Karolinska Institutet
Department of Neuroscience

Opponent:
Prof. Laura Calza
University of Bologna
Department of Pharmacy and Biotechnology

Examination Board:
Assoc. Prof. Arne Lowden
Stockholm University
Department of Psychology

Assoc. Prof. Catharina Lavebratt
Karolinska Institutet
Department of Molecular Medicine and Surgery
Division of Translational Psychiatry

Assoc. Prof. Rochellys Diaz Heijtz
Karolinska Institutet
Department of Neuroscience

“There are all sorts of interesting diseases out there, and lots of them are quite exotic – you’ve got elephant man syndrome and you’ve got progeria, which is the disease where you basically die of old age when you’re about 10 years old, and then you’ve got cannibals eating brains and getting prion diseases. And those are very exciting, and they are great and great junior high school papers about the disease and such… so there are all sorts of these great made-for-TV movie diseases out there.

But when you want to come to the basic meat and potatoes of human medical misery there is nothing out there like depression.”

- Robert Sapolsky

POPULAR SCIENCE SUMMARY OF THE THESIS

The hypothesis of developmental origins of health and disease posits that insult to normal development can lead to adult onset of disease. A large range of prenatal insults can affect the developing foetus such as, malnutrition, maternal diseases, exposure to toxic substances and stress. Increased levels of stress hormones (glucocorticoids) have been linked to increased risk of mental disorders including depression. Depression one of the leading causes of disability worldwide and it is estimated to affect ~300 million people. Considering the number of people affected by depression, the disorder is not only a major problem for the suffering patients and their families, but also an economic burden on society. Many depressed patients do not reach or maintain symptom remission. Often the efficacy of the treatment is low, and patients can go through multiple rounds of different treatments before they get a successful therapy. A major advance in treatment of depression would be the development of methods that could examine objectively individual patients and provide personalized therapy. The problem is that depression is a complex disorder no single cause and there are many possible risk factors, with no single cause or completely clarified underlying mechanisms. A lot of promising research is currently ongoing and will certainly expand our understanding of the disorder. My contribution is based on experimental studies on mice and investigations on depressed patients. I studied the development of a late onset depression-like behaviour in male mice subjected to prenatal stress. Male mice did not respond to classic first line of antidepressant drugs, but did respond to an alternative antidepressant called desipramine (DMI). Interestingly, depression was preceded by alterations of circadian activity and treatment with DMI early on could rescue the mice from circadian alterations and prevented the onset of depression. Female mice, on the other hand, exhibited behavioural features similar to the ones observed in models of attention deficit hyperactivity disorder (ADHD). Decrease signalling of the neurotransmitter dopamine pathway, which typically is the target of ADHD medication, accompanied the behavioural changes. The results from the experiments on mice emphasise the role of biological sex in the development of neurodevelopmental disorders. Both depression and ADHD show significant sex differences, not only in prevalence, but also in manifestation and underlying mechanisms. Most medical research is still being conducted only in male subjects, which may affect the development of medical treatments. My research findings highlight the need for inclusion of both sexes in medical research. Given the connection between depression, circadian alterations, and effects of antidepressant medication in our mouse model, I evaluated the circadian patterns of activity in patients suffering from depression. In depressed patients, I was able to fit symptom severity with patterns of activity, measured with wrist-worn actigraphs, which is a non-invasive method of measuring activity over several days. Finally in patients treated with internet-based cognitive behavioural therapy the response to treatment could be fitted by circadian features. While the sample size was small, the prospects of prediction of response to treatment may have large implications as it could potentially help clinicians in the prescription of a personalized therapy, thereby reducing the suffering experienced by patients.

ABSTRACT

Adverse conditions of different origin occurring during development can have a negative impact on the nervous system and increase risk for the onset of mental disorders. In mice prenatal exposure to excess glucocorticoids (GC) leads to late onset depression-like behaviour in males which is preceded by alterations in circadian entrainment. The aims of this thesis were to (1) identify sex-related differences in behavioural outcomes with a special focus on circadian activity and mood-related behaviours; (2) investigate the mechanisms behind the behavioural alterations; (3) implement novel computational techniques for characterisation of behaviour in rodents; and (4) explore the translation potential of the analysis of activity in patients suffering from depression. Pregnant C57Bl/6 were exposed to the synthetic GC dexamethasone (Dex) (0.05 mg/Kg/day, i.p.) from gestational day 14 until delivery. We analysed the behaviour of both males and female offspring at the age of 6 months focusing on circadian entrainment of spontaneous activity in the home cage environment. There were sparse differences between Dex and control (Ctrls) males at baseline, which were consistent with decreased social behaviour. In contrast, Dex-females were spontaneously hyperactive, a phenotype resembling ADHD models. Next, we investigated the changes in spontaneous activity following an abrupt advance in dark phase onset (phase shift). Dex-males re-entrained activity faster, while in Dex-females re-entrainment was delayed as compared to Ctrls. We implemented a multivariate approach to analysing the spatial and temporal organisation of behaviour which included affinity propagation (AP) clustering and uniform manifold approximation and projection (UMAP) using a set of 129 features extracted form activity recording. AP-clustering allowed the identification of features with similar patterns of variations following the phase shift, while UMAP supported the visualisation and quantification of changes in organisation of behaviour. The organisation of behaviour changed in both males and females, particularly in the dark phase. Dex-males displayed fewer, but more persistent alterations, while in Dex-females most alterations were transient and returned to baseline values within 5 days after the phase shift. The behaviour alterations in response to the phase shift pointed at alterations in the function of the central clock, the suprachiasmatic nucleus (SCN). In Dex-males the coupling between SCN and peripheral oscillators was disrupted, but was restored by enhancing GC receptor-mediated signalling by the antidepressant DMI. Furthermore, DMI also prevented the onset of depression. In Dex-females instead, the coupling between SCN and peripheral oscillators was preserved, supporting the idea that altered coupling is an early sign specific for depression onset. To investigate the connection between Dex-female behaviour and central clock alterations we performed gene expression analysis by RNA-sequencing followed by SPIA pathway analysis and identified significant alterations in glutamatergic, GABAergic, and dopaminergic signalling. We selected a set of relevant genes to validate the altered expression by cross-referencing differentially expressed genes in the SCN with the international mouse phenotype consortium (IMPC) database for associated phenotypes. Using this approach, we identified several differentially regulated genes supproting a decrease in dopamine signalling and the ADHD-like phenotype in Dex-females.

Spontaneous activity can be measured also in human subjects by means of actigraphy. We used actigraphy recordings from patients suffering from major depression to explore possible correlations between patterns of activity and symptom severity or response to internet-delivered cognitive behavioural therapy (iCBT) as antidepressant treatment. We implemented an independent homogenous training of model ensembles using systematic bootstrapping (with replacement) followed by pruning based on goodness-of-fit criteria. The aggregated output outperformed individual models by a factor of 4, indicating that ensemble training increases the accuracy of fitting. We further applied an external validation procedure using an independent dataset to provide proof-of-concept evidence for the possibility to model symptom severity estimated by MADRS-S. Our data suggests that higher symptom severity is associated with less complex patterns of activity, stronger coupling with circadian entrainers and less robust circadian rhythms, while larger improvement following iCBT is associated with less fragmented activity, more robust circadian rhythms, and higher day-to-day variability before treatment. To summarize, these studies suggest a strong connection between circadian activity and neuropsychiatric disorders. Further experimental and clinical investigations are needed to dissect all relevant systems and molecules involved to provide new insight into mental disorders.

LIST OF SCIENTIFIC PAPERS

I. Desipramine restores the alterations in circadian entrainment induced by prenatal exposure to glucocorticoids. Spulber S, Conti M, **Elberling F**, Raciti M, Borroto-Escuela DO, Fuxe K, Ceccatelli S. Translational Psychiatry. (2019) 9:263

https://doi.org/10.1038/s41398-019-0594-3

II. Sex-differences in long-term outcome of prenatal exposure to excess glucocorticoids – implications for development of psychiatric disorders. **Elberling F**, Spulber S, Bose R, Keung J, Ahola V, Zheng Z, Ceccatelli S.

(manuscript)

III. Patterns of activity correlate with symptom severity in major depressive disorder patients. Spulber S, **Elberling F**, Svensson J, Tiger M, Ceccatelli S, Lundberg J. Translational Psychiatry. 12, 226 (2022).

https://doi.org/10.1038/s41398-022-01989-9

IV. Development of an ensemble approach using circadian patterns of activity to model the response to cognitive behaviour therapy as antidepressant treatment – a pilot study. **Elberling F**, Raciti M, Ceccatelli S, Lundberg J, Spulber S.

(manuscript)

CONTENTS

1 INTRODUCTION 5
1.1 Developmental origins of health and disease 5
1.2 Glucocorticoids and the HPA-axis 5
1.3 Depression 6
1.3.1 The HPA-axis and glucocorticoid signalling in depression 7
1.3.2 The neuroplasticity and hippocampal neurogenesis hypothesis 7
1.3.3 Monoamine hypothesis 7
1.3.4 Antidepressant treatment 8
1.4 Circadian rhythms 9
1.4.1 Mood disorders and circadian rhythms 10
1.5 Sex differences 11
2 RESEARCH AIMS 13
3 MATERIALS AND METHODS 15
3.1 Mice (Paper I and II) 15
3.1.1 Model characterization (Paper I and II) 15
3.1.2 Animals and treatment (Paper I and II) 15
3.1.3 Treatment with Desipramine (Paper I) 15
3.1.4 Recording of spontaneous mouse behaviour in home cage (Paper I and II) 16
3.1.5 Behavioural analysis (Paper I and II) 16
3.1.6 Animal Sacrifice (Paper I) 20
3.1.7 Brain sectioning (Paper I) 20
3.1.8 RNA extraction and gene expression analysis (Paper I and II) 20
3.1.9 Analysis of clock gene expression in skin fibroblasts (Paper I) 21
3.1.10 State portraits and analysis of coupling between clock gene expression (Papers I and II) 21
3.1.11 Bulk RNA-sequencing (Paper II) 21
3.1.12 Selection of genes for expression analysis (Paper II) 22
3.1.13 Analysis of glucocorticoid receptor activation in the hippocampus (Paper I) 23
3.1.14 Analysis of dendritic arborization (Paper I) 24
3.1.15 Analysis of neurogenesis (Paper I) 24
3.1.16 Statistical analysis (Paper I) 25
3.2 Humans (Paper III & IV) 25
3.2.1 Patient recruitment and data collection (Paper III and IV) 25
3.2.2 External validation (Paper III) 26
3.2.3 Quality control and inclusion criteria (Paper III and IV) 26
3.2.4 Pre-processing and feature extraction (Paper III and IV) 27
3.2.5 Primary cultures of skin fibroblasts (Paper IV) 28
3.2.6 Model ensemble development (Paper III and IV) 29
4 RESULTS AND DISCUSSION 31

4.1 Mice (Paper I and II) 31
4.1.1 Behavioural alterations 31
4.1.2 Mechanistic aspects 34
4.1.3 General discussion 38
4.2 Humans (Paper III and IV) 41
4.2.1 Activity patterns and symptom severity 43
4.2.2 Molecular clock function 44
4.2.3 Activity patterns and the response to antidepressant treatment 44
4.2.4 General discussion and limitations 46
5 CONCLUDING REMARKS 49
6 ACKNOWLEDGEMENTS 51
7 REFERENCES 53

LIST OF ABBREVIATIONS

ACTH	Adreno Corticotropic Hormone
ADHD	Attention Deficit Hyperactivity Disorder
AVP	Arginine-Vasopressin
Bmal1	Brain and Muscle Aryl Hydrocarbon Receptor Nuclear Translocator-like 1
CA	Cornu Ammonis Area
CRH	Corticotropin Releasing Hormone
Ctrls	Control animals
DEG	Differently Expressed Gene
Dex	Dexamethasone
DMI	Desipramine
FLX	Fluoxetine
FST	Forced Swim Test
GC	Glucocorticoids
GD	Gestational Day
GR	Glucocorticoid Receptor
HCs	Healthy Controls
HPA	Hypothalamic-Pituitary-Adrenal
Hsp90	Heat Shock Protein 90
iCBT	Internet-delivered Cognitive Behavioural Therapy
LD	Light-Dark
MDD	Major Depressive Disorder
ML	Machine Learning
NE	Norepinephrine
Per #	Period Circadian Protein Homolog #
SCN	Suprachiasmatic Nucleus
SNRI	Serotonin-Norepinephrine Reuptake Inhibitor
SSRI	Selective Serotonin Reuptake Inhibitor

1 INTRODUCTION

1.1 DEVELOPMENTAL ORIGINS OF HEALTH AND DISEASE

The hypothesis of developmental origins of health and disease (DOHaD) had its beginning with Barker's investigations indicating that cardiovascular diseases in adult life may have their origin during development. Later studies have provided evidence linking adverse prenatal events with the occurrence of metabolic syndrome, asthma, cancers, osteoporosis, and neuropsychiatric disorders [1]. DOHaD theory posits that an adverse intrauterine environment alters the developmental trajectory, resulting in structural and functional changes in target tissues/organs [2]. For the central nervous system, the early period in the first 3 years of life is a critical developmental window, and insults can alter brain maturation with a subsequent negative impact on neuronal and neuro-glial connections that can affect normal brain functions. Factors affecting the maternal wellbeing throughout gestation (*i.e.*, placenta dysfunctions, stress, malnutrition, hypertension, diabetes, obesity, infections, and exposure to toxic insults) may have negative consequences on the foetus resulting in intrauterine growth restriction, prematurity, low birth weight and hypoxia, conditions that can critically influence the trajectory of the development of the nervous system shaping the future health of the individual.

1.2 GLUCOCORTICOIDS AND THE HPA-AXIS

Most prenatal adverse conditions are associated with high levels of glucocorticoids (GC) and considering that GC is critical for the normal development of many organs, including the nervous system, it is conceivable that alterations in their levels may result in long-lasting detrimental consequences.

GC are a class of steroid hormones secreted by the adrenal glands that have a critical role in mediating the stress response. In baseline conditions, GC is released in pulses of varying amplitude, with several peaks and troughs within a 24-h cycle. The hypothalamic-pituitary-adrenal (HPA)-axis regulates the release of GC. Briefly, the corticotropin-releasing hormone (CRH), released from the hypothalamus, signals the anterior pituitary gland to release adrenocorticotropic (ACTH) which controls the release of GC from the adrenal gland into the bloodstream. Interestingly, the response to ACTH signalling is gated by an internal mechanism which changes sensitivity to stimulation following a circadian pattern [3]. GC signalling is mediated by the GC receptors (GR). Circulating GC, by binding to GR, regulate HPA-axis functions via negative feedback loops closing at different levels (anterior pituitary and hypothalamus) [4]. CRH- and ACTH receptors have also a key role in regulating the axis. Hippocampal neurons express GR, and the hypothalamic secretion of CRH is also suppressed by inhibitory projections from the hippocampus [5]. When inactive, GR located in the cytosol, in heterodimer complexes including Hsp-90. Upon binding the ligand, GR homodimerize and translocate to the nucleus where it regulates gene expression by binding to GR-responsive elements (GRE) sequences in promoter regions. GR also interacts with nGRE (negative

GRE) where it recruits co-repressors resulting in gene repression. Accumulating evidence point at faster, non-genomic effects, mediated by membrane-bound or cytosolic GR [6,7].

In early developmental stages, GC induces cell proliferation, differentiation, and maturation during the organogenesis of kidneys, cardiovascular system, and gastrointestinal tract. GC support the organogenesis of the central nervous system by initiating terminal maturation of neural progenitors, remodelling of axons and dendrites, and promoting cell survival [8–10]. Essential for immediate postnatal survival, CG promotes lung maturation and initiates surfactant production [11–13], which lead to the use of synthetic GC administration to expecting women at risk of preterm delivery in order to diminish the risk of infant mortality [14]. Despite this short-term benefit of exogenous GC agonists, long-term risks of chronically altered HPA-axis response to stress were uncovered by epidemiological studies [15]. This has been confirmed in animal models that show decreased GR in the hippocampus [16] which results in HPA-axis hypo-responsiveness [17] and increased susceptibility of neuronal cells to oxidative stress associated with altered antioxidant defences [18]. The long-term effects of exposure to excess GC depend on the timing of exposure and involve epigenetic modifications which can be passed to the offspring [19,20]. In humans, conditions related to prenatal excess GC lead to intrauterine growth retardation (see [11]). Interestingly, low birth weight has been associated with a higher risk for attention-deficit hyperactive disorder (ADHD) [21,22], schizophrenia [23] and depression [24–26].

1.3 DEPRESSION

DSM-5 criteria for major depressive episode

1. Depressed mood most of the day, nearly every day
2. Markedly diminished interest or pleasure in all, or almost all, activities most of the day, nearly every day.
3. Significant weight loss when not dieting or weight gain, or decrease or increase in appetite nearly every day.
4. Insomnia or hypersomnia nearly every day
5. Psychomotor agitation or retardation nearly every day (observable by others, not merely subjective feelings of restlessness or being slowed down).
6. Fatigue or loss of energy nearly every day.
7. Feelings of worthlessness or excessive or inappropriate guilt nearly every day.
8. Diminished ability to think or concentrate, or indecisiveness, nearly every day.
9. Recurrent thoughts of death, recurrent suicidal ideation without a specific plan, or a suicide attempt or a specific plan for committing suicide.

Major depressive disorder (MDD) is a common neuropsychiatric disorder, often chronic or recurrent, with a significant negative impact on the overall health, as well as on social and professional functioning of the afflicted individuals. Persistent depressed mood or loss of

pleasure or interest in most activities are core diagnostic signs. The DSM-5 diagnosis criteria require 5 or more of the symptoms listed in the table above to be present simultaneously for at least two weeks, and "cause clinically significant distress or impairment in important areas of functioning". The aetiology of depression is largely unknown, and it is a heterogenous disorder (227 possible combinations of symptoms according to DSM-5 diagnostic criteria). There are several partly overlapping pathophysiological theories supported by experimental and clinical findings [28]. Following diagnosis, symptom severity can be assessed using different validated scales, designed either to be administered by clinicians, or as self-assessment tools. The Montgomery-Åsberg depression rating scale (MADRS) is a copyright-free scale [27], most widely used in Europe.

1.3.1 The HPA-axis and glucocorticoid signalling in depression

Experimental data indicated a bidirectional connection between depression and stress and GC secretion. Chronic stress leads to depression in both experimental models [29] and humans [30]. In addition, baseline GC secretion and the stress response are altered in depression patients [31] with distinct sex-differences in HPA-axis reactivity and stress generation [32]. In addition, developmental exposure to excess GC alters the function of the HPA-axis and induces late-onset depression-like behaviour in male mice [33]. Similarly, IUGR increases the risk of developing depression in adulthood [22,26,34–36].

1.3.2 The neuroplasticity and hippocampal neurogenesis hypothesis

Neuroimaging studies found consistent hippocampal atrophy in depression patients. Noteworthy, it is not limited to chronic or recurrent cases but is also found at disease onset (first depressive episode), which is consistent with a neurodevelopmental origin of depression [37]. Experimental models and post-mortem investigations have shown significant synaptic atrophy, as well as decreased hippocampal neurogenesis and altered dendritic arborization, which are consistent with cognitive impairment associated with chronic depression. Down-regulation of neurotrophins, such as BDNF and NGF, has been suggested to play a role in decreased neurogenesis and onset of depression-like behaviour. The neuroplasticity hypothesis is somehow filling the gaps in the alternative pathophysiological theories. Thus, it may explain the delay in onset of antidepressant effects of pharmacotherapy; effective antidepressants restore neurogenesis, and blocking hippocampal neurogenesis prevents antidepressant effects of SSRIs [38].

1.3.3 Monoamine hypothesis

The monoamine hypothesis has been developed starting from the finding that monoamine depletion by reserpine (an antihypertensive drug) induces depression, and drugs which increase monoamine (predominantly, but not limited to serotonin; see bupropion) levels in the brain are effective antidepressants (MAOI, SSRI, etc). Alterations in serotonin, norepinephrine and dopamine signalling have been suggested to contribute to depression symptoms based on the pharmacological profile of antidepressant drugs. While undeniably useful for drug development, the timing mismatch between pharmacological effect (minutes-hours) and the onset of antidepressant effects (days-weeks) indicates that the monoamine signalling hypothesis may be an oversimplification. The systematic umbrella review of evidence by Moncrieff et al. does not find support for the connection between decreased

serotonin signalling and depression, but finds only weak support for decreased serotonin concentration following long-term antidepressant use [39].

1.3.4 Antidepressant treatment

There are several antidepressant treatments available, including non-pharmacological interventions (*e.g.,* CBT, ECT) and pharmacotherapy. ECT has been used since the 1940s for both unipolar and bipolar depression. Seizures are induced by electrical stimulation of the brain under general anaesthesia, and a treatment cycle usually requires 6-12 administrations (2-3/week). It is currently the most effective antidepressant therapy (remission rate >50%), however, it is reserved only for the most severe cases or for treatment-resistant cases because of the risks associated with general anaesthesia. Pharmacotherapy was developed based on the monoamine imbalance pathophysiological hypothesis coined in the 1960s. Different antidepressant drug classes target serotonin, dopamine, or norepinephrine signalling, and have comparable clinical efficiency. The first line of antidepressant drugs are SSRIs, but the exact mechanism leading to symptom relief is not completely understood. Clinical practice shows that about 2/3 of patients respond to SSRI monotherapy, but only 1/3 reach remission. A characteristic feature of antidepressant pharmacotherapy is the slow onset of effects (typically 2-3 weeks). Recently, novel treatments include ketamine and psilocybin, which provide rapid and prolonged antidepressant effects after a single administration. CBT, developed in the 1980s and 1990s, builds on the hypothesis that symptoms and dysfunctional behaviours are mediated cognitively, therefore psychiatric conditions can be treated by modifying dysfunctional thinking. The clinical efficacy of CBT is comparable to pharmacotherapy (about 30%).

To date, there are no objective measures/biomarkers to predict the response to specific antidepressant treatment, and effective therapies are identified by trial and error. A recent extensive review analysing individual trajectories in response to treatment show that the patterns of response to treatment are consistent across drugs [40]. While successful antidepressant response can be predicted by clinical features, it is not possible to predict the specific antidepressant to which a patient will respond. Therefore, it is recommendable to search for predictors of meaningful response to specific treatments [40]. Guidelines for the treatment of patients with depression recommend a stepwise approach with CBT as the first line, followed by SSRIs (at least two different compounds), and SNRIs (at least two additional compounds) alone or in combinations.

Given the heterogeneity of depression presentation (reliance on subjective reporting of feelings and mood), it is not surprising that the development of experimental models of depression and relevant behavioural tests is a challenging task. However, proxy measures for the core symptoms have been developed in rodents, namely learned helplessness and anhedonia. The former is assessed by exposing the animal to an unescapable aversive situation, such as suspension by the tail (tail suspension test, TST), or immersion in a water-filled cylinder (forced swimming test, FST), then measuring the total time spent not trying to escape (immobility time). The latter is assessed by measuring the bias toward consumption of sweetened vs. regular water (sucrose preference).

1.4 CIRCADIAN RHYTHMS

Regulation of homeostasis in anticipation of the light/dark (LD) cycle is paramount for any organism, and it serves to function by not only adjusting the biological rhythms to the time of day but also by predicting the coming changes such as approaching light and dark period. Strong evidence suggests the age of the biological circadian clock is extremely old as it is observed in plants (folding or expanding leaves during the day), in drosophila (increased activity starting close to the beginning of dawn) and in mammals [41].

The biological molecular clock in mammals is comprised of several transcription factors engaged in interlocked feedback loops, generating self-sustained oscillations with a period of ~24 hours. It is estimated that up to 10% of genes expressed are displaying circadian oscillations, therefore disruption of the circadian clock can have extensive consequences within the organism [42]. Briefly: BMAL1 is constitutively transcribed and forms a heterodimer together with CLOCK which attaches to the E-box promotor element of DNA initiating transcription of target genes. The genes activated comprise the negative part of the feedback loop of the molecular clock consisting of PER (1-3), Cry (1-2), REV-ERB, and RORs. REV-ERB inhibits the transcription of BMAL1 and the heterodimer CRY1-PER inhibits BMAL1:CLOCK E-box transcriptional activity, thus creating the approximately 24-h period of gene fluctuation (Fig. 1-1). All cells have this internal biological clock, yet they are unable to keep the 24-h oscillations of the clock genes synchronised at population level. For instance, skin cells grown in culture over a few days will gradually lose the synchronisation of oscillations in clock gene expression. To keep the synchronisation with 24-h period, these cells require regular signals from a master clock [43,44]. In mammals, the central master clock consists of a population of neurons located in the suprachiasmatic nucleus (SCN) – hypothalamic nucleus located directly above the optic chiasm. SCN neurons are the only cells displaying an internal clock that oscillates without the need for constant entrainment. Clock genes in peripheral oscillators (cells outside of the SCN) are entrained by GC signalling (which upregulate the negative branch of the feedback loop). Notably, GR is not expressed in the SCN. The shell of the SCN releases arginine-vasopressin (AVP) into the paraventricular hypothalamic nucleus, regulating the release of CRH and thereby the rest of the HPA-axis, coupling peripheral oscillators to the SCN.

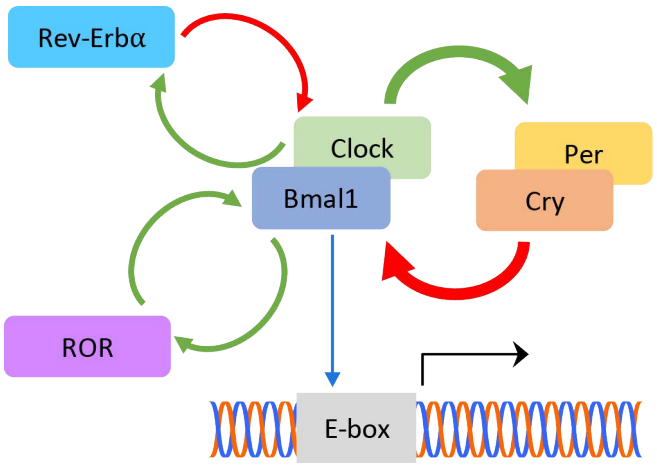

Figure 1-1 The core molecular clock machinery. The loop is initiated by spontaneous up-regulation of BMAL1 and CLOCK, which drives the expression of PER and CRY by binding to DNA at E-box sites. PER and CRY repress the expression of BMAL1 and CLOCK. Auxiliary loops involve REV-ERB and ROR.

The SCN acts as a pacemaker and entrains downstream peripheral oscillators, and the SCN must balance two opposing modes, strict control of the internal circadian rhythms but also be modifiable enough to adjust for changes in the environment. Several events occur at approximately the same time each day, and the SCN allows for proper timing of recurrent events such as feeding, sleep, etc. Strict control by the SCN keeps the circadian organization if the organism experiences small perturbations in the environment. However, the environment is not static and the SCN should be adaptable enough to accommodate these changes and entrainers are signals which influence the circadian rhythm within the SCN. Photic entrainment is the strongest circadian entrainer, particularly in rodents in laboratory conditions. The SCN is synchronized by light mediated through glutamatergic signalling from the retinohypothalamic tract (RHT) relaying light information directly from the retina. Different types of stimuli affect the circadian rhythm as well, such as feeding and environmental temperature, as well as social interactions (social entrainment, particularly relevant for non-solitary animals). Jetlag is therefore a transient condition generated by the mismatch of the internal circadian rhythm with the external natural LD cycle as well as the mismatch between different oscillators within the body as they do not entrain with the same speed. Jetlag is experienced when the body moves across time zones, and in humans, social jetlag is when social activities force the body out of the normal range of internal circadian rhythms [45–47].

1.4.1 Mood disorders and circadian rhythms

Depression is associated with disruption of sleep and alterations of circadian rhythms, and both shift-work and jetlag have been linked with an increased risk of depression [48,49]. The severity of depression symptoms is associated with the degree of misalignment of circadian rhythms, and post-mortem brains of people suffering from depression show disruption of clock genes [50]. In addition, several antidepressants produce changes in circadian features and some therapies involving chronotherapy and wake and light therapy have proven effective in certain cases [51,52]. Genetic association studies also identified links between clock gene variants and depression (PER2 [53]; CRY2 [54]; CLOCK [55,56]) and seasonal affective disorder [57]. In rodents, Bmal1 knock-down in the SCN [58], or manipulation of the LD cycle [59] can result in depression-like behaviour [60]. In human populations, circadian disruption by shiftwork was associated with an increased risk to develop depression [48]. A recent large population study indicates that blunted circadian rhythms of activity are associated with an increased lifetime risk for depression and mood instability (not satisfying the diagnostic criteria for unipolar or bipolar depression) [61].

Another relevant psychiatric disorder discussed in this thesis is ADHD which has also shown associations with circadian alterations. ADHD patients have observed later chronotype, as well as longer sleep latency and delayed dim-light melatonin onset. Furthermore, ADHD has blunted oscillation of core clock genes BMAL1 and PER2 and children with ADHD had observed blunted HPA-axis reactivity and decreased levels of circulating GCs. Finally, morning light therapy and sleep intervention both have shown a decrease in ADHD symptoms [62]. Methylphenidate, a common ADHD medication, increase the activity of the neuronal firing rate in the SCN in mice and induced a delay of the trough of the firing rhythm

together with a reduction in rhythm variability [63]. Taken together, these data point to the interlinkage of depression and ADHD with circadian rhythms, and understanding the connection between the two is an important point of investigation in the pursuit of future treatment of both disorders.

1.5 SEX DIFFERENCES

Historically neuroscience research has favoured a bias against female subjects. While in recent years this trend has decreased, many studies that include both sexes do not consider sex as an experimental variable and this concerns both animal and human research. Omissions of reporting the sex of the subjects studied are also widely observed in both rodent and human research. Moreover, sex is rarely considered in research based on *in vitro* cultured cells such as immortalized cell lines. Sex could be responsible of still unknown effects and if not reported or considered as a variable, the reproducibility of the studies may be drastically affected. Furthermore, the lack of inclusion of females leads to an underrepresentation of an entire segment of the population, which in turn, can negatively affect the progress in understanding diseases and in developing new treatment strategies. Sex has only been considered as an experimental variable in a few nervous system regions and functions, such as the hippocampus. Very little is known on specific effects of chromosomal sex, gonadal sex, hormones and environmental variables on sexual differentiation and adulthood, which leaves a gap in our understanding of a system as complex as the nervous system [64].

Among the most stable findings in psychiatry are the consistent results supporting sex related differences in mental disorders with regard to prevalence, symptomatology, risk and influencing factors and disease course. Women have a higher risk of being affects by mood and anxiety disorders, while men are more at risk of developing ADHD, autism, and late onset schizophrenic psychoses. The limited understanding of the processes leading to the observed correlations between sex and mental health problems. More research is needed because we do not know all mechanisms underlying sex influences on the nervous system and its disorders and without the inclusion of both sexes we may never know [65]. Hopefully the research conducted in this project will add another piece to this complex puzzle.

2 RESEARCH AIMS

The overall aim of the thesis was to investigate the effects of prenatal exposure to excess GC on circadian rhythms and explore potential translation towards clinical applications.

The specific aims of the studies were:

- To identify sex-related differences in behavioural outcomes with a special focus on circadian activity and mood-related behaviour
- To identify potential mechanisms for the observed behaviours
- To implement advanced computational techniques for characterisation of behaviour in rodents
- To explore whether the experimental findings may be relevant and applicable in clinical settings

3 MATERIALS AND METHODS

3.1 MICE (PAPER I AND II)

3.1.1 Model characterization (Paper I and II)

Our laboratory has previously characterized the consequences in mice exposed to Dex *in utero* during the last week of gestation. Both males and females had decreased body weight until postnatal day (PND) 28. Only Dex-males displayed impaired social behaviour up until 3 months and progressive alterations in photic entrainment of spontaneous activity consistent with a rather rigid circadian pattern (*e.g.*, late onset and early offset of active phase, delayed acrophase). The phenotype was established by 5 months of age, and was associated with blunted circadian oscillations in corticosterone secretion, and downregulated GR expression in the hippocampus. When challenged with a 6-h advance in onset of dark phase, spontaneous activity re-entrained to the new LD cycle almost instantaneously in Dex-males, while Ctrl-males took several days to adapt to the shifted LD cycle. By the age of 12 months, we could document the onset of depression like behaviour in FST and TST. In addition, we found hippocampal neurogenesis to be altered, with lower numbers and morphological alterations in newborn granule cells in the dentate gyrus. Finally, fluoxetine (FLX) treatment did not have antidepressant effects, while desipramine (DMI) reversed depression-like behaviour and restored hippocampal neurogenesis [33,66].

3.1.2 Animals and treatment (Paper I and II)

All experiments were conducted in agreement with the European legislation and Swedish national regulation following approval by the local Animal Ethics Committee (Stockholms Norra djurförsöksetiska nämnd).

Pregnant C57Bl/6NCrl dams (N = 5 animals/group) (CharlesRiver, SCANBUR Research, Sollentuna, Sweden) were injected subcutaneously with 0.05 mg/kg/day Dexamethasone (Dex) from gestational day 14 until giving birth, controls were injected with vehicle solution (10 ml/kg/day). On PND 3 the litter was culled to 4 pups per litter and at PND 21 weaned and injected subcutaneously with a radio frequency identification transponder (RFID) (Trovan™ Unique T-100A, Trovan, UK). The procedure was done under brief 4% isoflurane anaesthesia. Animals were placed in groups of 5 animals per cage, only housing same-sex animals together, with each animal originating from different litters.

3.1.3 Treatment with Desipramine (Paper I)

Animals received DMI (Sigma-Aldrich, Stockholm, Sweden) dissolved in drinking water (10 mg/kg/day) for 28 days starting at the age of 5 months. The treatment was continued during the recording of spontaneous activity. We have not observed changes in fluid intake during DMI treatment.

3.1.4 Recording of spontaneous mouse behaviour in home cage (Paper I and II)

Recording of spontaneous behaviour was done in GR900 cages (Tecniplast, Buguggiate, Italy) which were a bit larger than the normal GM500 cages in which the animals were housed in at the local animal facility. Animals were placed in a Scantainer (SCANBUR, Sollentuna, Sweden) and housed at 22 ± 1 °C; 50 ± 5 % relative humidity. The Scantainer located in an isolated room and interactions with researchers were limited to once per week for cage change (including water and food change) which was done during the light phase of the day.

Cages were placed on top of the TraffiCage system (New-Behavior, Zurich, Switzerland), two cages containing one Dex and one Ctrl group could be recorded simultaneously. The TraffiCage system comprised an array of five antennae located in a plate placed underneath the cage. With a resolution of 20 ms, the system allows for continuous recordings of all caged animals with time stamps and the location of all caged animals. Animals were placed in the Scantainer one week before the beginning of the recording session for full acclimatization and entrainment of the LD cycle. Animals were recorded for at least 3 days before the introduction of a 6-hour phase advance during the light sections of the day and recorded for at least 5 days after the phase shift.

3.1.5 Behavioural analysis (Paper I and II)

3.1.5.1 Detection of onset of active phase and assessment of photic entrainment (Paper I and II)

To identify the onset of the active phase, time series of activity counts were obtained and exported as ASCII files and analysed using custom algorithm implementations in Matlab™ (Version 9.3 and above; The MathWorks™, Natick, MD, USA). The activity was binned in 5 min non-overlapping epochs and smoothed by weighted average with a sliding Gauss window (2 h width). The epochs with activity higher than the individual's detrended average were considered "active" epochs. The active phase could be defined as a sequence of active epochs continuous or separated by gaps no longer than 1 h. The onset of the active period was defined as the time corresponding to the beginning of the active phase (relative to subjective time, ZT; ZT0 = light on). Spontaneous activity was defined as entrained to the LD cycle if the onset of the active phase occurred within 1 h from the onset of the dark phase. The time of re-entrainment was estimated when the individual's spontaneous activity was entrained to the shifted LD cycle induced by the 6-hour phase shift.

3.1.5.2 Analysis of periodicity and variability of spontaneous activity (Paper I)

Periodicity of spontaneous activity of animal behaviour was analysed using Lomb-Scargle periodogram in non-overlapping continuous 24 h epochs using a publicly available implementation of the algorithm in Matlab™. We analysed the variability of spontaneous activity throughout 96 h of continuous baseline recording and after phase shift by calculating intradaily variability (IV) and detrended fluctuation analysis (DFA). IV was calculated as the

ratio between average square differences between consecutive time bins (pooled activity over 5 min) and global variance over the entire epoch. IV generally ranges between 0-2, with low IV indicating smooth fluctuations in activity levels and higher IV indicating fragmented activity patterns characterized by abrupt transitions between active and inactive intervals. DFA yielded a scaling exponent calculated by linear regression analysis for residual variance in time after detrending against the time scale used for detrending. Detrending ranged from 20 min to 21.3 h (ultradian range) in equally spaced exponential increments. The correlation coefficient of linear regression in a double-logarithmic plot translates into a scaling exponent and describes the long-term autocorrelation patterns embedded in the time series. Complex time series with fractal-like patterned irregularity yield values between 0.5 and 1: positively correlated fluctuations yield a scaling exponent around 0.5: values around 1 suggest strong underlying regularity (such as diurnal rhythm); values approaching 1.5 indicate unbounded fluctuations resembling random walk (Brownian noise). The scaling exponent for spontaneous activity in young, healthy humans and rodents is approximately 0.8.

3.1.5.3 Analysis of behavioural features (Paper II)

The time series of activity counts were exported as ASCII files and analysed using custom algorithm implementations in Matlab™. To identify the onset of the active phase, the activity was binned in 5 min non-overlapping epochs and smoothed with a sliding Gauss window (2-h width). The epochs with activity above the animal's detrended average were considered "active epochs". The active phase was defined as a sequence of active epochs contiguous or separated by gaps no larger than 1 h. The onset of the active phase was defined as the time corresponding to the beginning of the active phase (relative to subjective time, ZT; ZT0 = light on). To locate the circadian peak of activity, the activity recording was smoothed with a sliding Gauss window spanning 243 consecutive bins (20.25 h) before identifying the daily maxima. The synchronisation of activity in group-housed animals we calculated the uncorrected coefficient of determination (Pearson, R^2) for linear regression of each animal's time series against the time series of the other animals housed in the same cage within 24-h intervals.

Further analyses based on the classification of visits and location within the cage were performed using a custom algorithm implemented in RStudio (version 4.0.5; RStudio, PBC, Boston, MA, USA). Recordings were first resampled at 1s resolution to align timelines across individual animals. To provide a consistent reference point for analysis of movement inside the home cage, we first identified intervals when all mice were detected by the same antenna and defined the antenna with the longest time spent together as the nest. The four other antennas were then annotated accordingly to their position in relation to the "nest" antenna as "adjacent", "across", "diagonal" and "middle". This was done for each LD cycle in order to capture potential relocations of the nest during the observation time. A "visit" was defined as the time interval spent by an individual animal in the detection area of a single antenna. To differentiate active visits from resting visits we applied a threshold. According to Blumberg et al [67], a threshold can be defined based on the distribution of visits. When visit duration is

plotted against frequency on a semi-logarithmic plot, inactive bouts would exhibit a linear distribution, whereas active visits would have an exponential distribution. The linear inactive part could then be determined through linear regression ($R^2 > 0.96$ and the standard deviation of slope < 0.05), enabling us to find the threshold between active and inactive visits (~7 min overall average). A sequence of visits below the threshold was then classified as an entire "trip", punctuated by "rest" intervals (above the threshold). We further sub-categorised the trip intervals and rests depending on their start and stop antenna. Rest intervals were either defined as occurring in the nest antenna or any of the other antennas (2 types), whereas trips started or ended in the nest or any of the other antennas (4 different types of trips).

We applied summary statistics (count, average, standard deviation, and skewness) for each light and dark section of each day, split into "trip" behaviours and "rest" behaviour. We also considered the time the mouse spent alone, with one other animal or with more than one animal. The trips were also classified based on the location of start and end antennas into four subtypes: trips: (1) starting and ending in the nest antenna (NN), (2) starting in the nest antenna and ending in one of the other four antennas (NR), (3) starting outside of the nest and ending in the nest (RN) and finally (4) starting and ending outside of the nest (RR).

This procedure generated 129 variables for each animal for each light and dark section per day. During the light section of the phase shift day, counts were multiplied by 2 to minimize the impact on downstream analysis since this day only yielded 6 h of behaviour on the subjective day. Each variable was then tested within each group to eliminate any features with no variance across groups. For downstream application, we defined the LD cycle of the advance in the onset of the dark phase as d0; we included 3 to 5 days before d0 to evaluate baseline behaviour, and 5 days (d1 to d5) after d0 to evaluate re-entrainment. The data was log-normalized [log10(1+variable)/10] before further calculations.

3.1.5.4 Affinity propagation clustering (Paper II)

Affinity propagation (AP) clustering is a clustering algorithm based on the concept of "passing messages between datapoints" which has the advantage of unbiased determination of both number of clusters and cluster composition [68]. The purpose of using AP-clustering was to identify consistent similarities between variables across groups, which can therefore be grouped in cluster, without necessarily assigning ethological interpretation to each cluster.

We averaged all features across baseline creating "baseline" behaviour, then we tested the difference across each of the 129 variables between Ctrls and Dex with a t-test. We applied AP-clustering on scaled data (package in RStudio) to identify behavioural phenotypes. The sample quantile (q) was set to 0.23 after an optimization step of choosing the value where the number of clusters was stable. We corrected the p-value within each cluster with FDR, revealing significant changes in individual behavioural features. To investigate the effects of phase shift on individual features we calculated the Z-score difference on each of the following days from baseline and used paired, two-sided t-test to measure the effects of phase

shift on behavioural features. To correct the p-value, we scaled all data and applied AP-clustering to determine within cluster FDR correction.

3.1.5.5 Uniform manifold approximation and projection (Paper II)

Uniform manifold approximation and projection (UMAP) is a non-linear dimensionality reduction algorithm which allows 2D visualisation of multidimensional data, in which distances between individual points are meaningful in relation to the actual distances in the features hyperspace [69]. Briefly, the resulting maps allow the quantification of differences between behaviour patterns considering all 129 variables.

In RStudio we applied the "umap" package after scaling the data to create UMAP coordinates using the following settings: nearest neighbours = 25; min dist = 0.3; number of components = 2; number of epochs = 500; and spread = 1. These values were selected after extensive testing across different parameter ranges to yield sufficient separation between light and dark behaviour on the UMAP coordinate map. The coordinates were used for downstream analysis of individual trajectories as follows: sequences of individual projections in the UMAP plane were analysed separately for light and dark. For each sequence, we computed a distance matrix between all points. We then estimated distances from baseline by averaging all distances between each point and baseline (Fig. 3-1).

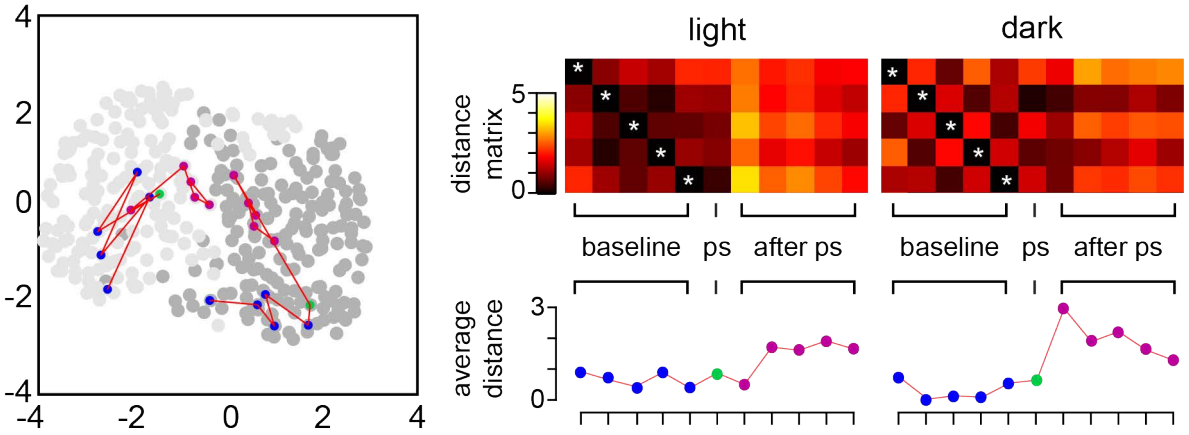

Figure 3-1 Illustration of the estimation of change in organisation of behaviour in response to phase shift. Asterisks indicate null distances, not used for calculation of baseline average.

3.1.5.6 Forced swim test (Paper I and II)

Depression-like behaviour was evaluated in the mice at the age of 6 and 12 months of age, by forced swim test (FST) as described earlier [33]. In brief, animals were placed individually in plastic cylinders (24 cm in height, 20 cm diameter) filled with water (23.5 °C) to a depth of 16 cm to avoid animals using their tails for touching the bottom of the cylinder. Animals were in the cylinder for 6 min and recorded during their whole stay. The recordings were analysed by an investigator blind to treatment and exposure. Immobility was defined as passive floating for at least 2 s. At the end of the recording, the animals were dried with paper towels

and returned to their respective home cage. The last 5 min of recording was used for quantification of immobility time.

3.1.6 Animal Sacrifice (Paper I)

Animals were sacrificed by an overdose of anaesthetic (sodium pentobarbital, 150 mg/kg) and perfused cardially with ice-cold buffered saline. Depending on the need brains were preserved in two different ways. For immunohistochemistry and qPCR following PBS perfusion, the animals were perfused with ice-cold 4% paraformaldehyde. The brains were removed and post-fixed with 4% paraformaldehyde overnight followed by cryoprotected first in 15% sucrose (followed by 30% sucrose when used for PLA) and frozen after they had sunk to the bottom and kept for later use. For nuclei isolation, the brains were removed after PBS perfusion and snap frozen on dry ice and stored at -80 ℃.

3.1.7 Brain sectioning (Paper I)

Brains used stereological counting of DCX+ cells were cut along the midline and the right hemisphere (injected with retroviral particles) was embedded in TopVision Low Melting Point Agarose (5% Thermo Scientific) and cut in 70 um thick coronal sections with a vibratome (Leica VT1000s) for confocal microscopy imaging. The left hemisphere was quickly frozen on dry ice, and 20 um thick sections were cut with a cryostat.

3.1.8 RNA extraction and gene expression analysis (Paper I and II)

For gene expression analysis with qRT-PCR analysis of SCN was done by dissecting a small piece of tissue (0.5 * 0.5 * 0.5 mm^3) from the anterior hypothalamus, posterior to the optic chiasm, lateral 0.5 mm on either side of the midline. The sampling could be verified by relative mRNA expression levels for *V1a* and *V1b* AVP receptors. The hippocampus was sampled by microdissection from frozen tissue. RNA was extracted with the FFPE RNA Purification Kit (Norgen Biotek, Montreal, Canada) according to the manufacturer's instructions. RNA concentration was measured on NanoDrop 1000 spectrophotometer (Thermo Scientific, Wilmington, DE, USA) and RNA degradation was assessed using an RNA 6000 Nano Kit (Agilent Technologies INC., Santa Clara, CA, USA) running on an Aglient 2100 Bioanalyser system (RIN range: 5.1-6.2). The RNA (1 μg template per sample) was reverse-transcripted into cDNA using 0.5 μg of oligo-dT primer according to the instruction of the Maxima First Strand cDNA Synthesis kit (Thermo Fisher). Amplification reactions were performed on a QuantStudio 5 thermocycler (Applied Biosystems) under the following conditions: initial denaturation 50 °C for 2 min followed by 95 ℃ for 10 min; followed by 40 amplification cycles (95 ℃ for 15 s, the annealing temperature 60 °C for 1 min). The specificity of the qRT-PCR reactions was evaluated by including a dissociation stage in the melting curve analysis. The mRNA expression was normalized against the housekeeping gene glyceraldehyde 3-phosphate dehydrogenase (*Gapdh*) and hypoxanthine phosphoribosyltransferase (*Hprt*) and the relative regulation was estimated using the $2^{-\Delta\Delta Ct}$ method.

3.1.9 Analysis of clock gene expression in skin fibroblasts (Paper I)

Tissue samples (~0.25 cm^2) were harvested from the ear of adult (6 mo) control and Dex-exposed mice under terminal anaesthesia. The tissue was rinsed in Hank's Balanced Salt Solution (HBSS) (Life Technologies Europe BV, Stockholm, Sweden), then minced with a sterile razor blade into Collagenase (Type XI-S) (Sigma-Aldrich, Sweden) (30 min at 37 °C). After digestion, 3mL of DMEM Medium (Life Technologies) supplemented with 10% Fetal Bovine Serum and 1% Penicillin/Streptomycin (Life Technologies) was added to a 6 cm plate and the samples were incubated at 37 °C for at least 6 days. After passaging (0.05% Trypsin-EDTA; Invitrogen), the cells were plated in 35mm dishes in MEF medium (DMEM Medium +10% FBS +1% pen/strep) at a density of at least 50 k/cm2. After 24 h, the expression of clock genes was synchronized by exposing the fibroblasts to 1 µM Dex. The cells were collected between 36 and 63 h after synchronization.

3.1.10 State portraits and analysis of coupling between clock gene expression (Papers I and II)

Animals were killed within an interval spanning 4.5 hours around the expected diurnal trough in *Bmal1* expression in the SCN (early subjective night). The relative mRNA expression for core clock genes *Bmal1* and *Per1* was normalized to the average of all samples before estimating the fold regulation using the $2^{-\Delta\Delta Ct}$ method. We assessed the coupling between oscillations in core clock gene expression using state portraits, where the state of an individual animal (data point) was described either by the expression of *Bmal1* and *Per1* in the same brain region or by the expression of *Bmal1* in two brain regions (SCN and hippocampus). Synchronized oscillations are defined as phase-locked oscillations, *i.e.*, they have the same period, and the time difference between the occurrence of peaks is constant. Under steady photic entrainment, when the oscillations in clock gene expression are synchronized, the state portraits approximate an arch of an ellipse, where the order of positions of datapoints follows the temporal sequence of sample collection. First, we assessed the synchronization of clock gene expression within the brain region by plotting the relative expression level of *Per1* against *Bmal1* mRNA in SCN and hippocampus, respectively. Second, we assessed the synchronization between the oscillations in *Bmal1* expression across regions by plotting the relative expression level of *Bmal1* mRNA in the hippocampus against the relative expression level in the SCN.

3.1.11 Bulk RNA-sequencing (Paper II)

Mice were sacrificed with an overdose of anaesthetic (sodium pentobarbital 150 mg/kg, i.p.) and perfused transcardially with ice-cold phosphate-buffered saline. The brains were removed and snap frozen on dry ice, then stored at –80°C. For the collection of SCN samples, the brains were placed in a cryostat (-25°C) for 30 min before the dissection to reheat. The SCN was dissected by needle puncture (diameter 1 mm; depth 1 mm) immediately caudal of the optic chiasm. Dissected tissue was placed for 20 min in hypotonic buffer N (10 mM Hepes pH 7.5, 2 mM $MgCl_2$, 25 mM KCl), and after placed in the Biomasher III (Nippi, Japan) for tissue homogenization. The flowthrough was collected after spinning down, then

added sucrose solution (2 M) and mixed gently. The solution was spun down (4 °C) at 6000 RFC for 10 min. The supernatant was removed, and nuclei were resuspended in ice-cold Buffer N (hypotonic buffer N, with 2M sucrose, 1 mM DTT and 1 mM PMSF) and spun down again for 10 min. Finally, the supernatant was removed, and the nuclei were resuspended in a freezing solution (3:7 buffer N in glycerol) and stored at -80 °C for further analysis.

RNA from isolated nuclei was extracted using Monarch RNA Miniprep kit (NEB, England), according to the manufacturer's recommendations. RNA concentration of each sample was measured using Qubit RNA Assay Kit with Qubit 2.0 Fluorometer (Life Technologies, USA). Then, cDNA sequencing libraries were constructed using Collibri 3' mRNA Library Prep Kit for Illumina (Invitrogen, USA) following the manufacturer's guidelines. Briefly, mRNA was reverse transcribed with oligodT primer containing an Illumina-compatible sequence at its 5' end. After the first strand synthesis RNA was removed by heat treatment, and second strand synthesis was initiated with random primers containing Illumina-compatible linker sequence at its 5' end. Finally, the libraries were amplified with Illumina's adapters for cluster generation and indices for multiplexing. Constructed libraries were quantified by qPCR using the Collibri Library Quantification kit (Invitrogen, USA) on StepOnePlus Real-Time PCR System (Applied Biosystems, USA). Paired-end reads of 150 bp long were generated on NovaSeq 6000 platform (Illumina, USA) at Novogene Bioinformatics Technology Co., Ltd., in Beijing, China.

The bulk RNA-sequencing identified 40.838 genes. We removed the genes labelled as clock-controlled genes (CCG) [http://cgdb.biocuckoo.org/download.php] to avoid false positive discoveries due to the desynchronization of the SCN between mice. On the remaining genes, we identified differentially expressed genes (DEGs) between control and Dex-female mice using the DESeq2 package and Wald test in RStudio. After FDR p-value adjustment we set a cut-off of adjusted p-value < 0.05 and |log2foldchange| > 1.5 as significantly changed genes (differentially expressed genes, DEGs). The DEGs were investigated with the signalling pathway impact analysis (SPIA) protocol. We identified 11 significantly changed pathways by Dex exposure corrected by FDR, out of which 6 pathways survived Bonferroni correction.

3.1.12 Selection of genes for expression analysis (Paper II)

We imported data from the International Mouse Phenotype Consortium (IMPC) to investigate the association between behaviour from known knock-out models, matching not only behaviour in our animals but also with the DEGs found in our dataset. Matching genes were further selected only if found in significant changed SPIA pathways and used for downstream qPCR. We also matched found DEGs with known ADHD genes from the website http://adhd.psych.ac.cn/LiteratureGene.do. From this list we also selected genes (Cnr1, Comt, Gsk3b, Th) as they are known to be associated with ADHD were used to investigate further candidate genes that could be used in the analysis. The genes were converted to mouse gene names and matched with any of our previously selected genes. Adding to this, three genes (Ciao3, Haghl and Stub1) from https://doi.org/10.1186/s12920-019-0593-5, were also

included in qPCR as these genes have been uniquely associated with ADHD in females and could be relevant for our experimental model.

3.1.13 Analysis of glucocorticoid receptor activation in the hippocampus (Paper I)

Inactive glucocorticoid receptor (GR) is located in the cytosol in a molecular complex built around the chaperone protein (heat shock protein 90, Hsp90). Upon binding to GC, GR is released from Hsp90 and translocates to the nucleus where it forms a homodimer that binds to the DNA and regulates gene expression. We quantified the GR complexes in the hippocampus was done by proximity ligation assay (PLA). After 30% sucrose solution the brain was snap-frozen in -55 °C isopentane before being sectioned 35 um of the hippocampal formation (-3.6 mm bregma). The sections were stored in Hoffman solution (250 ml 0.4 M PBS, ethylene glycerol 300 mL, 300 g sucrose, 10 g polyvinylpyrrolidone, 9 NaCl, high purity water to 1000 mL) and stored at -20 °C until PLA staining. Free-floating PLA was performed using the DUO92101 kit as instructed by the manufacturer. The sections were washed 3 * 5 min in PBS, followed by 20 min of quenching in 10 mM glycine (Sigma-Aldrich), then washed 2 * 5 min in PBS. The sections were then permeabilized with 0.1 % Triton X-100 for 30 min in a blocking buffer (SuperBlock, Thermo Scientific). The sections were incubated with primary antibodies diluted in blocking buffer overnight at 4 °C, the following antibodies: mouse monoclonal anti-GR (1:100, SAB4800041), rabbit polyclonal anti-GR (1:50, sc-8992) and rabbit polyclonal anti-HSP90 (1:25, SAB4300541). The following day the sections were washed 2 * 5 mi min blocking buffer and transferred to a 37 °C humidified chamber with the probes (1:5, PLA Probes) for 2 hours. Afterwards, the sections were washed 2 * 5 min under gentle agitation first in blocking buffer, then in PBS. Sections were incubated with hybridization-ligation solution (1:5, Ligation Stock (5x) in dH_2O, 1:40, Ligase (1 U/µL)) for 1 hour in a 37 °C humidified chamber. The sections were washed twice in Buffer A (8.8 g NaCl, 1.2 g Tris base, 0.5 ml Tween 20 in 1000 mL water adjusted to 7.4 pH with HCl), before incubation with a rolling circle mixture (1:5, Amplification Stock (5x) in dH_2O, 1:80, Polymerase (10 U/µL)), for 100 min in 37 °C humidified chamber. The sections were then washed 2 * 10 min in Buffer B (5.84 g NaCl, 4.24 g Tris base, 26 g Tris-HCl in 1000 mL water adjusted to pH 7.5 using HCl), shielded from light at room temperature under gentle agitation, and then mounted on microscope slides with mounting medium (Mounting medium with DAPI, Doulink, Sigma-Aldrich), coverslipped, sealed with nail polish and stored at -20 °C until imaging. The PLA signal was detected using Leica TCS-SL confocal microscope (Leica) and quantified with Duolink Image-Tool 1.0.1.2 (Sigma-Aldrich). A stack of 20 adjacent optical slices (1 µm thick) was acquired for blue (DAPI) and red (PLA) channels. The PLA signal was visible as intense spots located in the cytosol or inside the nucleus. The images used for analysis were generated from the red channel by maximum projection intensity of confocal stacks. We estimated the signal density within manually delineated regions of interest (ROI) inside the pyramidal cell layer of the hippocampal CA as the proportion of area occupied by the red signal after applying a threshold. 3 images per area for each animal (N = 4 animal/ group)

was used to derive the average signal density in the hippocampus and was used for subsequent analysis.

3.1.14 Analysis of dendritic arborization (Paper I)

The maturation of newborn granule neurons was investigated in cells expressing green fluorescent protein (GFP) delivered using a retroviral vector injected stereotactically in the dorsal hippocampus as described earlier [66]. The injection site was located as follows, in relation to bregma: anteroposterior, −2.6 mm; mediolateral, +1.75 mm; dorsoventral, −2.0 mm (from dura). The GFP-expressing cells were analysed 4 weeks after the injection, which corresponds to the full morphological maturation of the retrovirus labelled granule cells (21–28 days post-infection). For the morphological analysis, all brain sections from the hemisphere injected with retroviral particles through the entire hippocampus (12–15 sections/animal) were collected in PBS for 10 min washing, and subsequently processed for free-floating immunohistochemistry as described above. Sections were then mounted on Microscope Slides cut edges frosted (VWR International) with Fluorescent Mounting Media (DAKO). We used rabbit anti-mouse GFP (1:1000, Thermo Fisher; USA) and PierceTM Donkey anti-Rabbit IgG (H + L). Cross Adsorbed Secondary Antibody 543 (1:200, Thermo Fisher; USA). An average optical thickness of 50 μm was imaged (from the slice thickness of 70 μm). Z-series at 1 μm intervals were acquired with a Plan-Apochromat 20 × 0.75 objectives, digital zoom 1.5, on a Zeiss ZEN 2009 LSM 510 META confocal system. A total of 5–12 cells from each mouse were analysed for each data point. All images were analysed in FiJi using a semiautomatic procedure. Images of dendritic arborization were deconvolved with an Iterative deconvolve 3D plugin and manually traced with the Simple Neurite Tracer plugin before running automated Sholl analysis. Granule cells displaying truncated dendrites, or grossly departing from the plane of the coronal sections, were excluded from the analysis. The number of neurons analysed ranged between 4 and 12/animal (N = 7–12 animals/treatment). The relative expression of Bmal1 was assessed by qPCR with GAPDH as a housekeeping gene. Circadian oscillations in clock gene expression were analysed using cosinor rhythmometry.

3.1.15 Analysis of neurogenesis (Paper I)

Neurogenesis and the maturation of newborn neurons were analysed as previously described in mice aged 6 or 12 months [66]. Briefly, proliferating of neuronal progenitors was labelled by 5-ethynyl-2 deoxyuridine (EdU) uptake. EdU (50 mg/kg/day) was injected i.p. for 5 consecutive days before killing the animals at 6 months. The EdU uptake was visualized using the Click-iT™ EdU Alexa Flour™ 488 Imaging kit (Thermo Fisher) as instructed by the manufacturer. Postmitotic progenitors committed to the neuronal lineage were identified in 12 months animals by immunohistochemical detection of DCX expression. The number of EdU or DCX-positive cells in the subgranular zone was assessed on a 20 μm thick frozen coronal section collected every 200 μm from the left hemisphere (*i.e.*, not injected with viral particles). The slices were mounted on SuperFrostPlus™ Microscope Slides (VWR International) and circled with a Dako pen. After 10 min re-hydration with phosphate-

buffered saline (PBS), sections were treated with a blocking mix (PBS, 5% Normal Donkey Serum, 0.3% Triton-X) for 2 h. Sections were then incubated overnight at 4 °C with primary antibody. After washing with PBS 3 × 5 min, sections were incubated with secondary antibody for 2 h at room temperature. After washing 2 × 5 min with PBS, sections were counterstained with 4′,6′- diamidino-2-phenylindole (DAPI, 1:1000, Sigma-Aldrich) for 5 min, washed with PBS for 3 × 5 min and mounted with coverslips. The primary antibody used was: the Guinea pig anti-mouse DCX antibody (1:1000, Millipore; CA). The secondary antibody used was Donkey anti-Guinea pig 488 (1:200, Alexa). The DCX-positive cells in the granule cell layer of the DG were counted throughout the entire hippocampal structure in a stereological design on equally spaced 20 µm sections (200 µm between consecutive slides). The total number of cells was estimated by multiplying the number of counted cells with the inverse sampling fraction.

3.1.16 Statistical analysis (Paper I)

All statistical analyses were performed in Statistica™ 13 (TIBCO Software Inc., Palo Alto, CA, USA). The onset of the active phase and the variability in spontaneous activity were analysed using a mixed model ANOVA with repeated measures, followed by Dunnett's post hoc test against Dex as the reference group. mRNA expression was analysed first by a one-sample t-test vs. "no-regulation" value (= 1), and then between-group comparisons were analysed by a two-sample t-test. The time to re-entrain and immobility time in FST and PLA group differences were analysed using simple ANOVA models followed by Dunnett's post hoc test against Dex as the reference group. The differences between Sholl curves were reported only when pointwise differences (t-test) were found significant for at least three consecutive points. Differences are reported as significant at $p < 0.05$. All individual comparisons are one-sided. The data are shown as average ± SEMPLA staining and quantification

3.2 HUMANS (PAPER III & IV)

3.2.1 Patient recruitment and data collection (Paper III and IV)

The training dataset was collected as part of the previously published study on serotonin transporter availability in patients given internet-based Cognitive Behavioural Therapy (iCBT) for the treatment of a major depressive episode [70]. Briefly, 17 subjects were recruited by advertisements in local newspapers. Diagnosis of depression was established after a full psychiatric assessment by a psychiatrist or by a resident physician supervised by a senior psychiatrist. The study included patients with an ongoing major depressive episode according to DSM-IV criteria, with a history of at least one prior episode and that was not undergoing any psychopharmacological treatment for MDD. Eligible patients had a MADRS score between 18 and 35. Control subjects had no history of psychiatric illness and matched the patients by age, sex, and intellectual ability [70]. The activity was recorded in 12 subjects for at least 7 consecutive days immediately before starting the CBT treatment program, (11 patients after completing iCBT (8 patients have been recorded both before and after treatment), and

16 healthy controls were used in Paper IV). Actigraphy recordings were acquired using GENEActiv Original wrist-worn actigraphs (Activinsights, Cambs, UK). The devices use three-dimensional accelerometers (dynamic range up to 8*g*; 12-bit encoding, resolution 3.9mg) at a 30Hz sampling rate to record wrist movement. The patients were instructed to wear the actigraph continuously on the wrist of the non-dominant arm and not remove it unless for personal safety reasons *(e.g.*, sauna, or contact sports such as martial arts, rock climbing, or volleyball). The raw data was downloaded using proprietary software, then processed in Matlab™ (The Mathworks, Natick, MD, USA), using a modified version of the code (https://github.com/DavidRConnell/geneactivReader), as described earlier [71]. Briefly, the Euclidean norm of change in acceleration vector was first smoothed using a rolling Gauss window spanning 30 consecutive datapoints (1s), then a high-pass filter was applied (threshold: 20mg = 196 mm/s^2) before computing the sum of changes in acceleration vectors over 1 min epochs (1440 samples/24 h). A total of 12 recordings spanning between 6 and 12 consecutive days were included for further analyses.

3.2.2 External validation (Paper III)

The external validation was performed on an independent dataset. The test dataset consisted of actigraphy data recorded as part of a clinical study addressing the effects of ketamine on serotonin receptor binding in patients with treatment-resistant depression [72]. Briefly, the study included 39 patients with an ongoing major depressive episode, with MADRS ≥ 20, resistant to selective serotonin reuptake inhibitor (SSRI) treatment in an adequate dose for at least 4 weeks. Ongoing antidepressant treatment was discontinued and actigraphy data were collected after a washout period of at least 5 times the half-life of the SSRI. The patients were instructed to wear the actigraph continuously on the wrist of the non-dominant arm and not remove it unless for personal safety reasons. The recording started before the first ketamine infusion and continued for the duration of the ketamine treatment program. For this study, we cropped the recordings to include the period immediately before the first ketamine infusion (*i.e.*, after drug washout period). Actigraphy recordings were acquired using Actiwatch 2 wrist-worn devices (Philips Respironics, Murrysville, PA, USA) set to record activity only integrated over 1 min epochs. The raw data was downloaded according to the manufacturer's instructions (Actiware 6.0.9, Philips Respironics) and then exported as text files. The text file was imported to Matlab™ using a custom function designed to yield an output similar to the one generated by the import function for GENEActiv devices. A total of 23 recordings spanning between 2 and 7 consecutive days were included in the test dataset.

3.2.3 Quality control and inclusion criteria (Paper III and IV)

The quality control was performed by the same observer, blind to group belonging. All recordings were first inspected visually using a standardized procedure designed to identify stretches of missing data, artefacts, and gross abnormal circadian patterns of activity (*e.g.*, shift-work, or other consistent activity at night). Intervals containing suspected shift-work (not reported at the time of recording), potential artefacts, or missing data, were cropped out. Individual recordings were included after cropping if they fulfilled the following

requirements: minimum recording length of 5 days; the recording did not include exceptional events with potentially high impact on the subject's circadian patterns of activity (as identified on the actigraphy recording); the recording was continuous and did not include stretches of missing data longer than 2h, regardless the reason to not wear the device and finally MADRS > 40 were excluded in Paper III, given the MADRS maximum in the training dataset was 35. Each recording included in subsequent analyses originated from different subjects (*i.e.*, only one recording per subject).

In the test dataset for Paper III, recordings were rejected for the following reasons: MADRS > 40 (1); recording length < 5 consecutive days (7); shift-work during recording time (2); missing data (2). This yielded a total of 24 recordings to use for further analyses: 12 for train and 12 for test datasets. In Paper IV, this procedure yielded a total of 28 recordings to use for further analyses: 16 for healthy controls, 12 for MDD patients before treatment (MDDpre) and 11 for MDD patients after treatment (MDDpost).

3.2.4 Pre-processing and feature extraction (Paper III and IV)

All processing of actigraphy data was performed in Matlab™ using custom implementations of publicly available algorithms. Movement probability density functions (PDFs) were calculated for each subject-day (*i.e.*, a complete sequence between consecutive midnights) by normalizing the activity count in each 1-min bin to the total activity counts for the corresponding 24-h period. This allowed comparisons between circadian profiles by eliminating the effect of variable total activity counts across days, subjects, and groups [73]. Group-wise differences between circadian profiles were evaluated using the Jaccard distance, which estimates the ratio between non-overlapping area and total area under the profiles. The Jaccard distance can assume extreme values of 1 (no overlapping) and 0 (perfect overlapping) and was preferred based on its intuitive geometrical correspondence [73]. The Jaccard distances from the healthy controls' profile were calculated over incremental time shifts between -12h and 12h. This was only applied in Paper IV.

For an in-depth analysis of patterns of activity, we first cropped all recordings between the first and last recorded midnight to yield an integer number of 24-h periods. The features we extracted describe the regularity, fragmentation, and complexity of circadian patterns of activity. The following features were extracted: circadian period; circadian peak and trough; relative amplitude [61,71,74]; scaling exponents [75]; intradaily variability; interdaily stability [76]; day-to-day variability. In addition, we included features describing the oscillations in clock gene expression in skin fibroblasts.

The circadian period was estimated using the Lomb-Scargle algorithm optimized for Matlab™ implementation [77]. The Lomb-Scargle periodogram was preferred over the most commonly used Sokolove-Bushell algorithm [78] because the latter has been shown to yield period estimates biased towards periods below 24h [79]. The circadian period was calculated over the entire recording using an oversampling factor of 10 to yield a resolution of the estimated in the range of minutes. The scaling exponent for detrended fluctuation analysis

was calculated for the magnitude of measured activity in 1-min bins using boxes equally spaced on a logarithmic scale between 4 min (4 consecutive samples) and 24 h (1440 consecutive samples) as described by Hu et al. [75]. The scaling exponent is a feature of the intrinsic regulatory mechanisms controlling the rest/activity patterns. It is not sensitive to extrinsic factors the subject is exposed to in normal daily activity but is altered as a result of disease [75,80,81]. Intradaily variability estimates the fragmentation of activity patterns by calculating the ratio between mean squared differences between consecutive time intervals and the mean squared difference from global mean activity per interval; it increases when the frequency and the magnitude of transitions between rest and active intervals are high, and decreases when active and inactive intervals consolidate[74]. Interdaily stability evaluates the coupling between activity patterns and circadian entrainers and is calculated as the ratio between variability around the circadian profile and global variability. High values indicate consistent activity patterns across days, consistent with a strong coupling between activity and circadian entrainers. The relative amplitude of circadian rhythms of activity (RA) estimates the robustness of average circadian rhythms [61,82]. The range of RA is bounded between 0 (no circadian rhythms) and 1 (robust circadian rhythms, with consistent timing of consolidated rest interval longer than 5h across days). The day-to-day variability comprised 3 features as follows: mean difference between consecutive days (rmssd), calculated as Euclidean distance between consecutive days, normalized to the total number of samples per day; average deviation from circadian profile (rmsmd), calculated as the Euclidean distance between each day and the average profile, normalized to the total number of samples per day; and the normalized difference between consecutive days (ddv), calculated as the ratio between mean difference between circadian profiles of consecutive days and mean deviation from average circadian profile.

Circadian profiles were calculated after normalization to the total amount of activity to isolate the distribution of activity from the confounding effects of variations in the total amount of activity across days. Instead, the variations in the total amount of activity were included in the estimation of day-to-day variability in addition to the (particularly in rmssd and rmsmd), and there was a good correlation between day-to-day variability measures calculated before and after normalization to total daily activity (not shown). To avoid redundancy, the final selection for building the feature space included only day-to-day variability measures before normalization.

3.2.5 Primary cultures of skin fibroblasts (Paper IV)

A skin biopsy (about 5 x 2 mm) was collected from the internal aspect of the arm under sterile conditions after local anaesthesia using EMLA patches (AstraZeneca, Södertälje, Sweden). The wound was then covered with a sterile patch, and a small scar was formed typically within 6-12 h. The tissue sample was quickly transferred to ice-cold HBSS (Life Technologies Europe BV, Stockholm, Sweden) and minced with a sterile razor blade into Collagenase (Type XI-S) (Sigma-Aldrich, Sweden) (30 min at 37 °C). After digestion, 3 ml of DMEM Medium (Life Technologies) supplemented with 10 mM Hepes buffer, sodium

pyruvate, non-essential amino acid mixture, Glutamax, 20% Fetal Bovine Serum, and 1% Penicillin/Streptomycin (all supplements were from Life Technologies) was added to a 6 cm plate and the samples were incubated at 37 °C until the fibroblasts reached confluence (typically 3-4 weeks). The confluent fibroblast cultures were passaged (0.05% Trypsin-EDTA; Invitrogen) and then plated in 12 multi-well plates at a density of at least 50 k/cm^2 in the same medium as used above. After 24 h, the expression of clock genes was synchronized by the addition of Dex to the culture medium to a final concentration of 1 μM. The cells were collected at 12, 15, 24, 27, 36, and 39 h after synchronization. The sampling scheme was designed to (1) avoid the first 12 h after synchronizations when the expression of clock genes was reset and has not yet initiated the self-sustained 24 h cycles of oscillation; (2) cover more than 24 h (assumed circadian period), and (3) reduce the bias towards assumed 24 h and capture slopes presumably more accurately than by sample collection at equally spaced time points. The relative mRNA expression of *BMAL1* and *PER2* was assessed by qPCR with *GAPDH* as a housekeeping gene. The relative mRNA expression was calculated using the $2^{-\Delta\Delta Ct}$ formula using the average of all samples per subject as reference. Oscillations in gene expression were analysed using the single component COSINOR method [83] assuming a 24 h period. The amplitude and phase angle for individual clock genes, as well as the difference in phase angle between the two genes, were included in the models.

3.2.6 Model ensemble development (Paper III and IV)

We implemented an ensemble approach for the prediction of response to treatment. We generated the initial ensemble by independent homogenous training using a systematic bootstrapping (with replacement) scheme for selecting up to 6 predictors/models. This approach ensured a minimum of 2 subjects/predictor[84] (MDD, N = 12), while systematically testing all possible combinations of predictors. After completing the generation phase, the models were annotated to facilitate separate analyses for ensembles with and without clock gene expression features. The separation was possible due to the independent homogenous training scheme. The model ensembles were pruned using the following criteria for retaining individual models: VIF < 5 (to avoid multicollinearity issues); R-square > 0.5 (the model explained > 50% of the variance in response); and RMSE < 3 or RMSE < 10% for symptom severity and response to treatment, respectively.

For Paper III, we then performed an external validation of filtered models. To this end, we evaluated the performance of models validated as described above on an independent (test) dataset. The performance of individual models was assessed using the coefficient of determination (R-squared), and the RMSE for predicted vs. observed MADRS to evaluate the precision and the accuracy of the estimate. We filtered the models to be further analysed as follows: significant correlation between predicted and observed MADRS ($p < 0.05$ corresponding to Pearson $R > 0.576$) and RMSE < 3 for the test dataset. To provide an internal reference for model performance, we generated a dummy model (predicted score = average score for the test dataset), and a random prediction dataset (1 million simulated sets of random integer values in the same range as the test dataset). The frequency of occurrence

for individual predictors in validated models was calculated as the number of models including each unique predictor divided by the total number of validated models for each level of complexity. The average frequency for the most common predictors was calculated as the average occurrence for each level of complexity. This approach compensates for the fact that the number of validated models increases dramatically with the number of predictors included. The leverage of individual predictors in each model was evaluated using the standardized coefficients for each model.

Finally, for Paper IV, we calculated the aggregated outcome by averaging per subject the output of all models. The ensemble performance on the dataset was evaluated using the root mean squared error (RMSE) as a measure of accuracy. To evaluate the performance of individual features across models, we calculated the coefficient of variance (CV) as the ratio between the standard deviation and the average of standardized coefficients for individual predictors. These parameters were calculated cumulatively over ensembles including models yielding an accuracy below or equal to 10% in 0.5% increments. The minimum accuracy of 10% was chosen using the following reasoning: the MADRS score after treatment is linked to the response to treatment modelled by the following formula: MADRSpost = MADRSpre x (1 + Response). Therefore, errors in the estimation of the MADRS score after treatment are proportional to the MADRS score before treatment and the error in the estimation of response to treatment. For reference, we used the minimum change of ~2 in the MADRS score that is relevant for the evaluation of response to treatment [85]. We then estimated the maximum error in aggregated output that would yield an estimated MADRS score after treatment within 0.75 points from the true value.

4 RESULTS AND DISCUSSION

4.1 MICE (PAPER I AND II)

4.1.1 Behavioural alterations

Our group has previously reported that 12 months-old Dex-exposed male mice exhibit depression-like behavior associated to impaired hippocampal neurogenesis, and blunted circadian oscillations in GC secretion. The analysis of spontaneous activity showed that progressive alterations in circadian entrainment preceded depression-like behaviour, and that the phenotype was already established by the age of 6 months [33]. In Paper II we tested both Dex-exposed male and female mice at the age of 12 months. Surprisingly, we observed sex-related differences in the responses in the FST: Dex-females exhibited shorter immobility time as compared to Ctrls while Dex-males displayed an increase in immobility time, in agreement with our earlier observations (Fig. 4-1 A). When we assessed the spontaneous activity in the home cage at the age of 6 months, it became evident that Dex-females had increased total number of visits per day as compared to Ctrls, opposite to Dex-males (Fig. 4-1 B). These findings prompted further investigations in both sexes focusing on differences in behavioural phenotypes and underlying mechanisms that may carry relevant translational aspects.

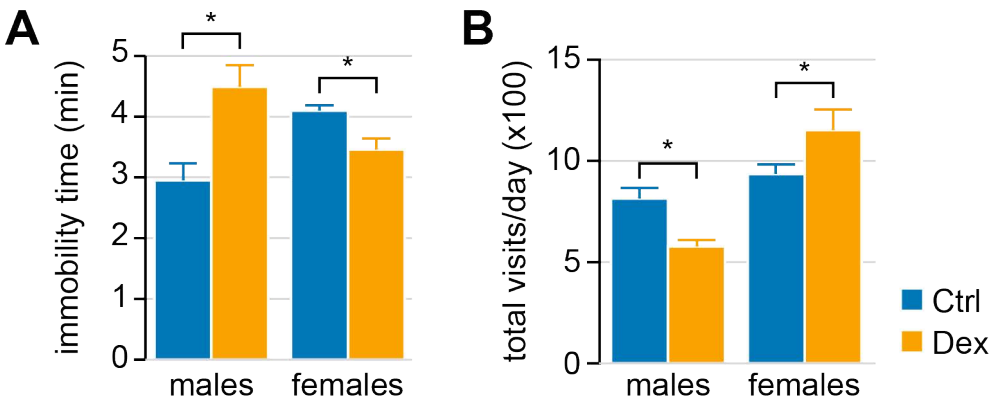

Figure 4-1 Sex-dependent outcomes of prenatal exposure to Dex in male and female offspring. (**A**) FST results in males and females tested at the age of 12 months. (**B**) Estimation of global activity over 24 h at the age of 6 months. Note the different outcomes of prenatal exposure to Dex in males vs. females.

4.1.1.1 Circadian entrainment of spontaneous activity (Paper I and II)

We subjected both sexes to a 6-h phase advance of the dark period and investigated circadian re-entrainment of onset and the circadian peak of spontaneous behaviour. Dex-males displayed a faster re-entrainment of activity onset, but not of circadian peak of activity as compared to Ctrls. Unlike males, Dex-females had a slower re-entrainment of onset of activity, and the location of the circadian peak was oscillating significantly during the period of re-entrainment.

Social interactions can synchronise activity in group-housed animals, provided the SCN function is preserved [86,87]. We calculated the coefficient of determination for linear regression of individual mouse activity against the activity level of all other cage-mates and used it as proxy measure for social entrainment. At baseline we found no difference between Dex-males and Ctrl-males, but Dex-females displayed stronger social entrainment, as indicated by a higher coefficient of determination as compared to Ctrls. Following the phase shift, social entrainment decreased significantly only in Ctrls, and the decrease persisted until the end of the observation period. In contrast, females exhibited only transient deviations from baseline immediately after the phase shift (Ctrl – increase; Dex – decrease), then returned to baseline.

The observation that social environment may have been altered by advancing the onset of dark phase inspired the following investigation. Mice typically display clear preference for a specific area in the cage which they use for nesting, and over several days we have observed that the location of nest area is very stable throughout the period of monitoring spontaneous activity in our experimental setting (unpublished observation). We therefore investigated the nest location within the cage, by measuring the amount of time spent simultaneously by all animals in area covered by each antenna. The location of the nest changed after the phase shift only in Ctrl animals in both sexes. Conversely, Dex-exposed animals remained at their previously selected location, although Dex-females changed location during baseline observation time. These findings highlight the significance of identifying the nest area as ethologically relevant reference point. In the feature extraction procedure, we used the nest area for classification of trips and geographic distribution of resting time.

4.1.1.2 Organization of spontaneous activity in the home cage (Paper II)

We extracted 129 features from the recording of spontaneous activity, which we used for describing the organisation of behaviour during light and dark phases, respectively (matching sets of features were extracted for each light and dark phase separately). At baseline, Dex-males display sparse differences from Ctrls, however consistent with the decreased social behaviour [33]: less resting bouts and total duration of rest in the nest area in both subjective day and night. In contrast, Dex-females covered longer distance, had longer distance per trip but shorter trip duration, and increased activity in the centre of the cage in dark, and had higher number of inactive visits in light (Fig. 4-2). This indicates unstimulated hyperactivity and fragmentation of rest intervals, a pattern of behaviour associated with ADHD. Baseline hyperactivity in familiar environment is particularly interesting, since it is a phenotype rarely reproduced in ADHD experimental models [88].

To evaluate the changes in organisation of behaviour following the phase shift, we first used AP-clustering to identify and analyse together features with similar patterns of variation across groups, without necessarily assigning ethological interpretation to each cluster. We observed an overall larger effect on behaviour during the dark phase in both sexes, and females displayed in general larger changes in behaviour as compared to males. The patterns of changes appear more persistent (*i.e.*, did not return to baseline by the end of the recording period) in males than in females, where most features returned to baseline by the end of the

observation period. This was particularly noticeable in clusters #1 and #2 in females, where a prominent number of features went back to baseline after re-entrainment. Interestingly, the highest number of significant alterations in dark phase occurred during the first day after phase shift (d1) and appeared to persist for longer in Dex-females as compared to Ctrls.

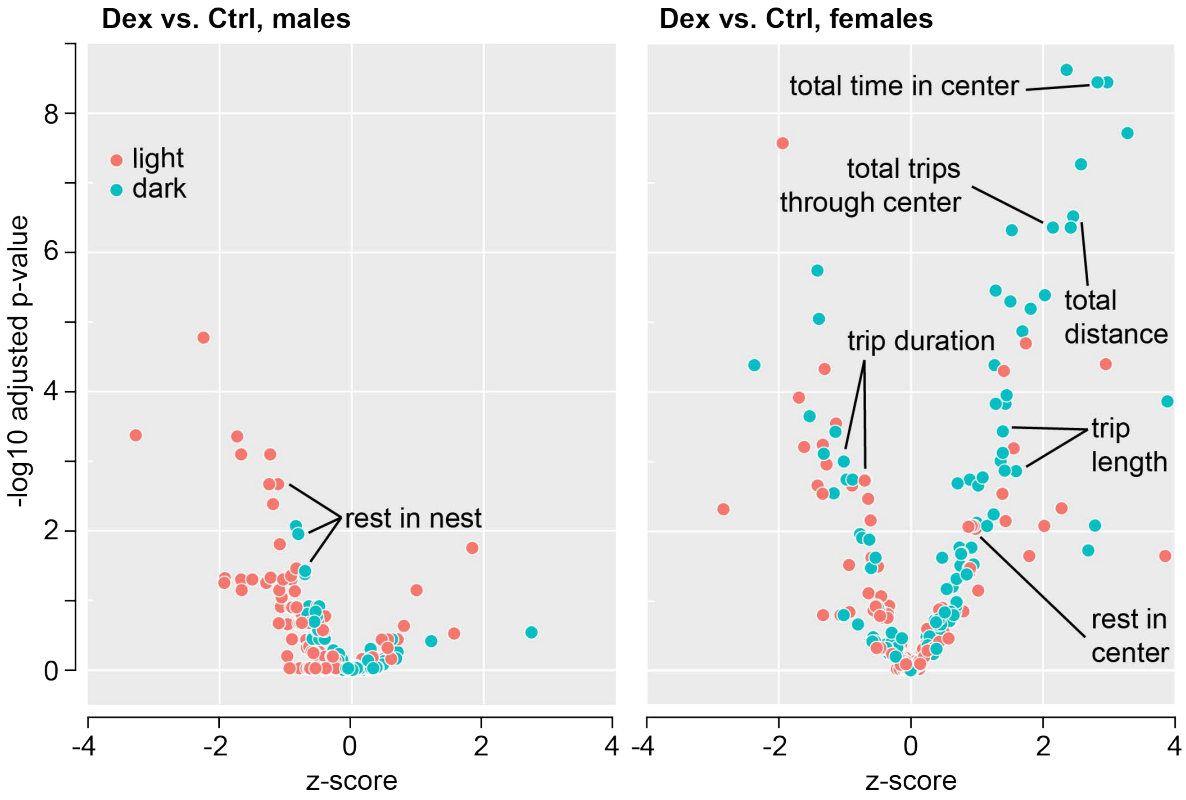

Figure 4-2 Changes in Dex-exposed animals' features compared to Ctrls at baseline. Note the number and magnitude of significant changes observed in females compared to males.

Next, we applied uniform manifold approximation and projection (UMAP) to the behavioural features for dimensional reduction to evaluate the effects of advancing the dark on the following light and dark phases. The 2D map generated a clear separation of light and dark behaviour across both sex and exposure. In males, the separation between groups at baseline was clear during the subjective day, but not during subjective night. After phase shift, Ctrls-males relocated to different region within the UMAP projections map, in both light and dark, while Dex-males appeared to only relocate during the subjective night. In females, a similar separation of baseline behaviour was observed in both groups, especially during the day. After phase shift, Ctrl-females' behavioural changes in both light and dark suggest a reduction in differences between the light and dark phase, *i.e.*, Ctrl-females less distinct from each within the UMAP coordinate system. Dex-females showed minor relocation in both light and dark, which was not marked by a similar reduction in the distance between light and dark behaviour (Fig. 4-3). The UMAP 2D mapping allows the estimation of distances between individual data points as Euclidean distances in the UMAP plane. We calculated a matrix of distances between each point and the baseline for each subjective day and night for each animal. In males, Ctrls displayed persistently increased distance from baseline starting at

phase shift day (d0) in both light and dark phases. In contrast, Dex-males exhibited virtually no change from baseline in the light phase, and a delayed (starting on d1) persistent deviation in the dark phase. This is consistent with the qualitative observation of differential relocation in the UMAP plane described above. In females, we found significant differences from baseline starting earliest one day after phase shift (d1), as indicated by the AP clustering analysis. Dex-females deviated from baseline only on d1 for both light and dark phases, while Ctrls diverged significantly from baseline for 3 consecutive days only in light phase.

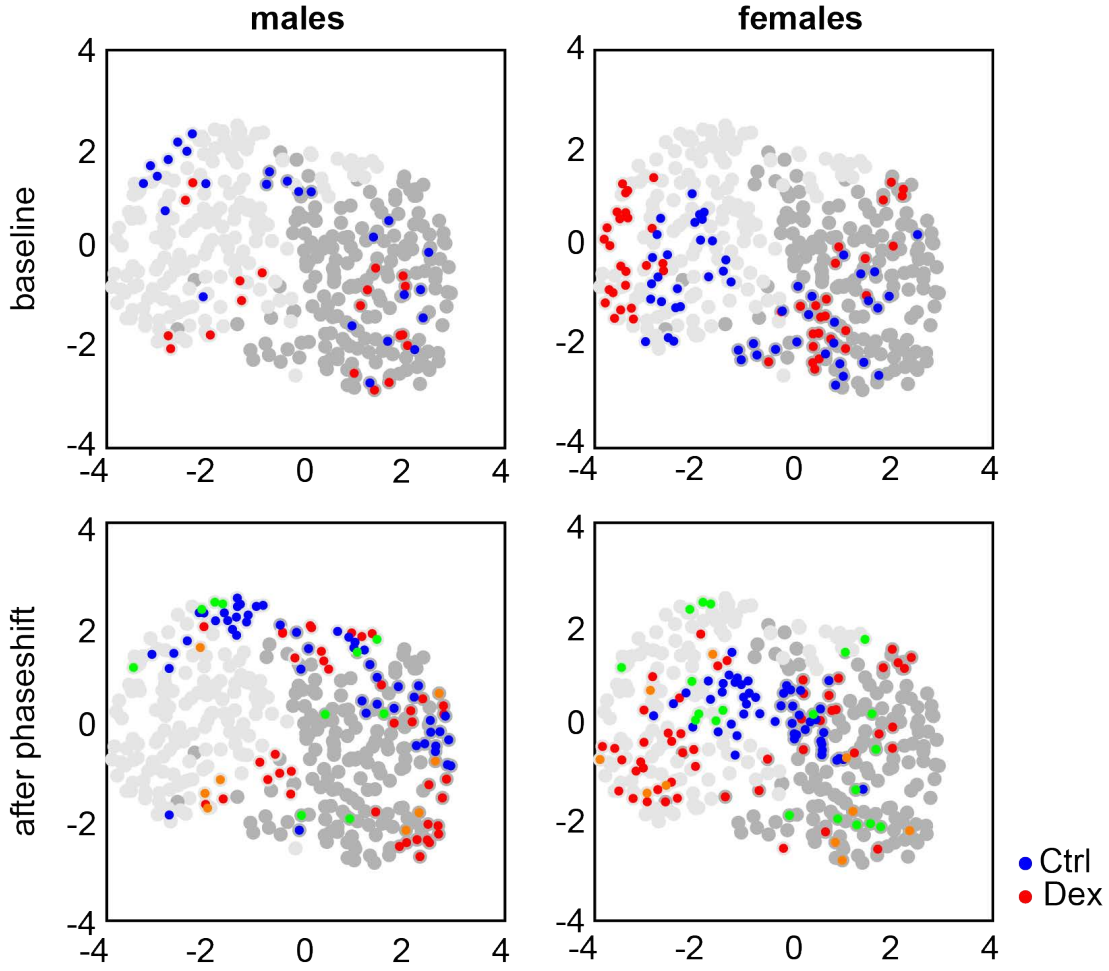

Figure 4-3 UMAPs of males and females, before and after phase shift. Light grey symbols depict the light phase (subjective day), dark grey symbols depict the dark phase (subjective night). Phase shift day is marked by green and orange for Ctrl and Dex, respectively. Distances between points reflect the degree of similarity between individual activity patterns.

4.1.2 Mechanistic aspects

4.1.2.1 DMI restores coupling between SCN and peripheral oscillators in Dex-males

Male mice exposed to Dex *in utero* do not respond to FLX, but DMI is effective in reversing the depression-like phenotype [33,66]. Notably, FLX requires rhythmic GC secretion for its antidepressant effects [89], while DMI enhances GR-mediated signalling [90,91]. This points to potential alterations in HPA-axis function in our model, and is supported by the blunted difference between peak and trough GC secretion [33]. AVP from the SCN signals the

hypothalamic paraventricular nucleus to stimulate the release of CRH, which further stimulates the release of ACTH increasing GC secretion by the adrenals. We found lower expression of *Avp* in the SCN, which suggests weaker circadian drive of HPA-axis. In addition, we found downregulated *GR* mRNA expression in the hippocampus, suggesting weaker negative feedback on HPA-axis. This is in line with the alterations in rhythmic secretion of GC documented earlier and may account for the uncoupling of oscillations in clock gene expression between SCN and hippocampus. We therefore treated Dex-males with DMI at the age of 6 months (*i.e.*, before the onset of depression-like behaviour), because it has been shown previously to enhance GR-mediated signalling [90]. We found that DMI treatment significantly delayed in re-entrainment and stabilized intrinsic rhythmicity in Dex-males. Thus, while naïve Dex-males lost circadian periodicity for about 3 days after phase shift, circadian periodicity was restored immediately after phase shift in DMI-treated Dex-males. We also investigated the variability in locomotor activity by means of DFA (scale-dependence) and IV (short-term variability, indicative of fragmentation of activity). The scaling exponent and IV were higher at baseline, and increased after phase shift in naïve Dex-males. In contrast, DMI treatment decreased both scaling exponent and IV at baseline and attenuated the effects of phase shift, suggesting consolidation of spontaneous activity and dampened acute change in response to phase shift, a pattern closer to Ctrl-males.

Next, we investigated the effects of DMI on SCN and the downstream coupling with peripheral oscillators. DMI treatment upregulated *Avp* expression in the SCN, which allows for stronger regulation of the HPA-axis by the SCN. We also found that *GR* expression in the hippocampus was upregulated in Dex-males after DMI treatment. GR exists in two forms, an inactive form, a heterodimer comprised of GR and heat shock protein 90 (Hsp90) found in the cytoplasm. When GC enters the cell, GR forms as a homodimer and translocates into the nucleus where it regulates gene expression. We used PLA to label GR dimers and differentiate between active and inactive forms. In naïve Dex-males we found lower levels of active GR homodimers than in Ctrl-males, and DMI treatment increased both cytosolic (inactive) GR-Hsp90 heterodimers, and nuclear (active) GR homodimers. This suggests stronger negative feedback signalling for the HPA-axis, which would strengthen the coupling between SCN and peripheral oscillators. Indeed, we found that the coupling of oscillations in clock gene expression in the hippocampus with the SCN was restored in DMI-treated Dex-males, which is in line with the delayed re-entrainment and consolidation of spontaneous activity as compared to naïve Dex-males. Furthermore, the amplitude of oscillations in clock gene expression in primary fibroblast cultures was higher in cells derived from DMI-treated Dex-males as compared to naïve Dex-males.

Lastly, we investigated the effects of DMI treatment at 6 months on depression-like behaviour and neurogenesis at the age of 12 months. At 6 months of age, Dex-males do not display depression-like behaviour (*i.e.*, increased immobility time in FST), nor is hippocampal neurogenesis altered as compared to Ctrls. However, by the age of 12 months, the depression-like phenotype is not present in Dex-males treated with DMI at the age of 6 months as in naïve Dex-males. Thus, DMI-treated Dex-males do not show increased

immobility time in FST, and hippocampal neurogenesis was not altered: the number and morphology of newly generated neurons (dendritic arborisation and proportion of V-shaped neurons) was similar to Ctrls. Taken together, these data indicate that DMI treatment prevents or delays the onset of depression-like behaviour in Dex-males.

4.1.2.2 Decreased dopamine signalling in the SCN in Dex-females

Opposite effects on circadian entrainment between males and females exposed to Dex *in utero* suggest different outcomes in males and females regarding central clock function. The coupling between *Bmal1* and *Per1* molecular clock in the SCN was preserved in both males and females, suggesting that photic entrainment was not affected by Dex-exposure. When we assessed the coupling between the SCN and peripheral oscillators (in this case the hippocampus), where the HPA-axis plays a critical role, we found that coupling was only lost in Dex-males, while in Dex-females was preserved (Fig. 4-4).

However, the response to phase shift revealed differences between Dex-females and Ctrls, suggesting alterations in central clock function We analysed gene expression in the SCN by means of bulk RNA-sequencing. Out of the initial 40 838 genes identified by sequencing we removed clock-controlled genes and found 2 312 differentially expressed genes (DEGs; 935 up-regulated) after correcting for FDR. The DEGs were further investigated using gene ontology (GO) term analysis, which yielded the most enriched terms of biological processes: cell morphology; neuron development; and regulation of nervous system development. Of the top 5 GO terms, two clusters were associated with neuronal development and synapse organisation and another cluster was involved with cell projection organization. We applied

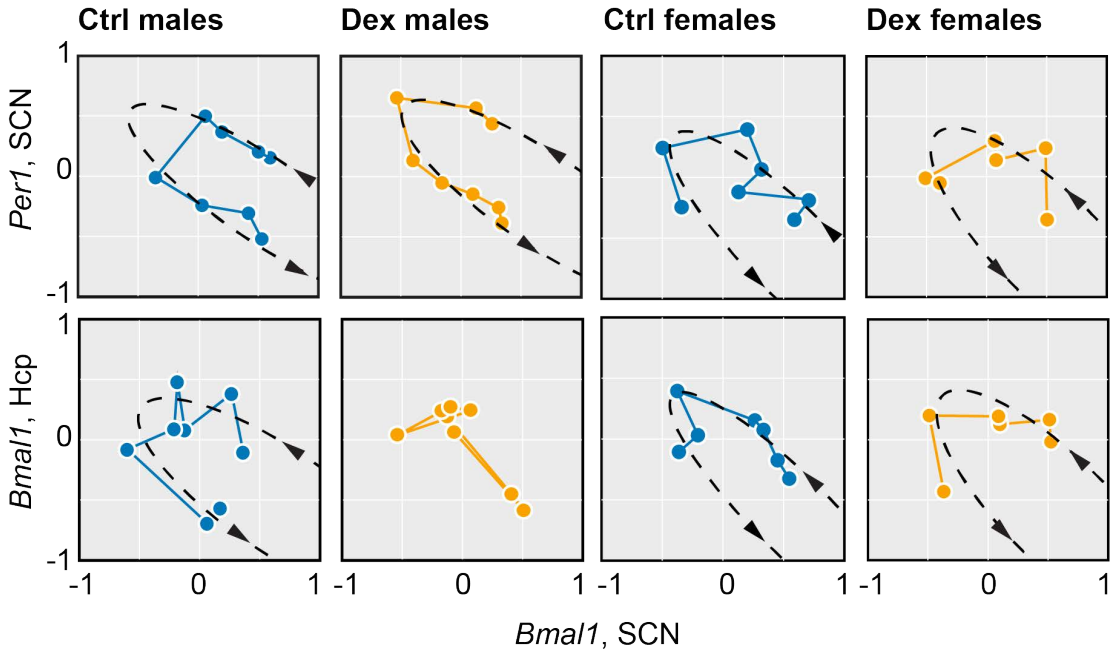

Figure 4-4 Comparison between photic entrainment of the SCN (top panels) and downstream coupling of peripheral oscillators (bottom panels) in males and females. Note that downstream coupling is preserved in Dex-females, but not in Dex-males.

SPIA analysis, which revealed 6 significantly changed pathways surviving Bonferroni correction: Alzheimer's disease; glutamatergic synapse; dopaminergic synapse; GABAergic synapse; long-term potentiation; and Parkinson's disease. We next used the international mouse phenotype consortium (IMPC), from where we selected genes with associated phenotypes resembling behavioural findings in our model, focusing in particular on genes relevant to dopaminergic signalling pathway and ADHD. The genes selected from the IMPC database were matched with the most prevalent genes highlighted by the SPIA analysis and with genes found in a database ranking genes associated with ADHD based on validation in published studies (see Table 4-1). Lastly, we have also used the list of differentially methylated genes identified in neural stem cells exposed to Dex [92].

Table 4-1 DEGs found in RNA-seq in Dex-females, relative to Ctrls. Green blocks under SPIA pathways show if genes were found within glutamatergic, dopamine and GABAergic pathways. Green blocks within ADHD and IMPC, indicates whether genes were observed in the IMPC database and ADHD gene list. qPCR presents directionality of gene expression in the SCN and the hippocampus, green indicates similar direction and red opposite direction from RNA-seq results.

DEGs, RNA-sequencing				SPIA pathways			ADHD	IMPC	qPCR	
gene	counts	change	p-adj	Glu	DA	GABA			SCN	Hcp
Gnao1	3677	-0,5	0.002							
Cacna1b	828	0,5	0.011							
Gabra2	649	0,6	0.006							
Cnr1	304	0,6	0.012							
Comt	680	0,4	0.025							
Kcnj6	477	0,7	0.000							
Gria1	3965	-0,4	0.016							
Th	119	-1,6	0.000							
Narfl	26	0,5	0.236							
Stub1	10	-0,2	1.000						↓	↑
Haghl	0	0	NA						↑	↓
Gsk3b	0	0	NA						↑	↑
Fmr1	121	0,9	0.012							
Pp1a	42	0,2	0.756						↑	↓
H2afz	847	-0,5	0.023							
Trpm1	2	-0,1	NA						↑	↓

We hypothesized that transcriptional changes induced by Dex exposure would result in similar differential gene expression patterns in other brain regions. To test this hypothesis, we measured the mRNA expression by means of qPCR on in tissue samples from SCN and hippocampus. Differential expression of individual genes matched 73,3% between SCN qPCR and SCN bulk-sequencing and 47,1% between hippocampus qPCR and SCN bulk-sequencing and finally 50% between the SCN and hippocampus qPCR (see Figure 4-5). Notably, baseline hyperactivity was consistently represented in the phenotypes associated with the genes with matching regulation within the SCN and the hippocampus (mapping in

quadrants I and III in Figure 4-5). Exposure to Dex induces persistent DNA hypomethylation in rat cortical neural stem cells, and we could document similar effects in the cortex of 3 days-old male pups exposed to Dex *in utero* [92]. Therefore, epigenetic changes may underlie the converging differential expression we observed in some genes. The contribution of epigenetic changes to the overall phenotype in females, however, needs further investigation.

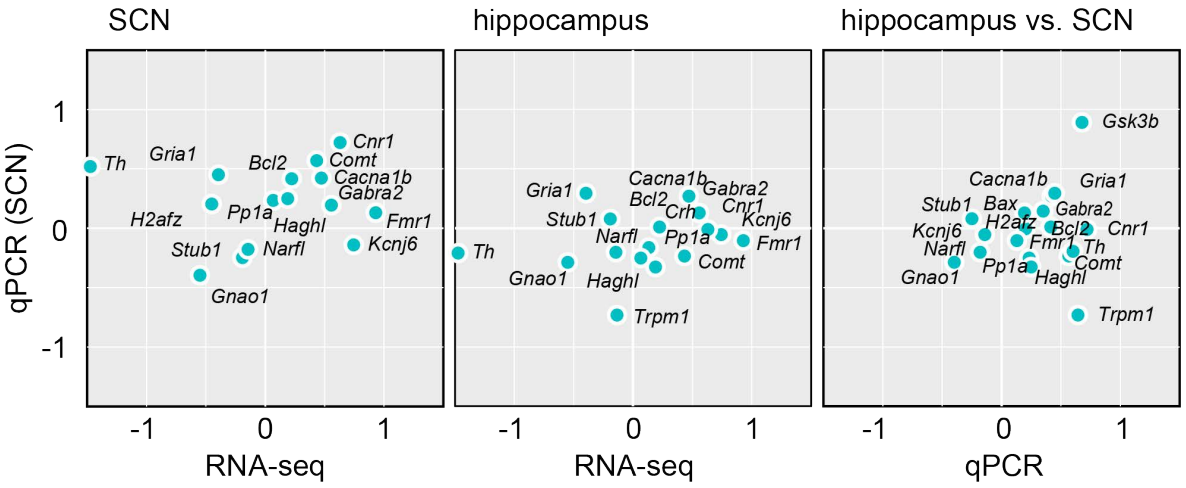

Figure 4-5 Matching differential gene expression between SCN and hippocampus. Panels 1 and 2: comparison between qPCR results from the SCN and the hippocampus with the results from bulk RNA-seq. Panel 3: comparison between differential gene expression measured by qPCR in the SCN and the hippocampus.

4.1.3 General discussion

Our studies have shown that *in utero* Dex-exposure has sex-dependent long-term effects on mice offspring: Dex-males develop late-onset depression-like phenotype, while Dex-females exhibit a hyperactive behavioural phenotype resembling the one observed in murine ADHD models. Underlying mechanisms may include sex-dependent alterations in the SCN and circadian entrainment-related mechanisms.

We investigated home cage spontaneous activity which can be divided into two different categories: static (baseline) characterized by constant light/dark cycle and dynamic, following the advance in the onset of the dark phase (adaptive, response to challenge). We can distinguish the first light-dark cycle after the phase shift as an additional special condition, because it is the first occurrence of an earlier dark onset, which presumably has the highest impact on organisation of behaviour. Remarkably, each condition contributes different information to the overall picture. We observed, for instance, that the differences between males at baseline are sparse, but the challenge of adaptation to advancing the onset of dark phase revealed differences leading to identification of mechanisms underlying the response to antidepressant treatment. In contrast, the differences between females at baseline revealed spontaneous hyperactivity, and the pattern of re-entrainment provided functional support for a mechanism suggested by gene expression analysis, namely altered dopamine signalling.

We investigated re-entrainment of spontaneous activity and dynamic changes in the organization of behaviour during subjective night (active phase) and subjective day (inactive phase) following the phaseshift. Darkness allows nocturnal animals, like mice, to become active, but does not necessarily induce activity, while light inhibits spontaneous activity. Thanks to the internal clock, mice can predict the time of transitions and change behaviour accordingly (anticipatory behaviour). After an abrupt change in timing of transitions between light and dark, the mice essentially need to adapt and re-align the internal clock to the new LD-cycle (re-entrainment). A relevant technical aspect is that hard boundaries were drawn between subjective day and night before running the feature extraction procedure and that the features are summary statistics which do not consider temporal sequences. Therefore, leakage of behaviours specific to a subjective phase into neighbouring opposite phase can account for deviations from baseline. This is particularly relevant for slower re-entrainment, as we found in Dex-females.

We used the onset and peak of activity to assess re-entrainment, and in this case masking, which is defined as a behavioural response to stimuli in the environment (*e.g.*, light-dark transitions, social interactions, restricted feeding, etc.) can obscure the onset of active phase. In our experimental setting, positive masking is represented by locomotor activation upon turning the light off, and negative masking is illustrated by the suppression of activity by turning the light on. In Dex-males masking seemingly plays an important role in photic re-entrainment, since the re-entrainment of both onset and the circadian peak of activity follow similar timelines, and the delay between onset and the circadian peak is constant. After the phase shift, re-entrainment in Dex-males is accompanied by isolated changes in the organization of behaviour, as detected by the analysis of deviations from baseline after AP-clustering. In contrast, masking is virtually absent in females after phase shift. In Ctrl-females re-entrainment of both onset and circadian peak of activity share similar timelines (as illustrated by the constant delay between onset of the circadian peak of activity), which is accompanied by larger deviations from baseline than observed in males during both subjective day and night. In contrast, in Dex-females, the re-entrainment of the circadian peak of activity is delayed compared to the onset of activity suggesting a robust drive of the internal clock on spontaneous activity. This is supported by the clock gene expression analysis in females, which indicates preserved photic entrainment and robust coupling between the SCN and peripheral oscillators, and contrasts with the observations of altered downstream coupling in males.

The first LD-cycle (*i.e.*, the subjective night with earlier onset and the following subjective day) is particularly interesting since it includes the first occurrence of light offset and onset with different timing. The most prominent effect is the change in coefficient of determination. A drop in coefficient of determination can be due to variability in individual reaction to the change in timing of light-dark transition, suggesting weaker social entrainment. In contrast, an increase in coefficient of determination suggests a synchronized reaction to sudden changes in environment (such as earlier timing of light-dark transition). In this case positive masking (synchronised increase in activity immediately after turning the light on, without

necessarily initiating the active phase) can increase the coefficient of determination, as observed in Ctrl-females.

Dex-males display accelerated re-entrainment, and similar phenotypes have been described after knocking out the expression of AVP receptors in the SCN [93,94], or by disrupting GC signalling [95–97]. Interference with AVP signaling weakens the coupling among different populations of neurons within the SCN and make the circadian timekeeping system more sensitive to perturbations, while disrupting GC signalling weakens the coupling between SCN and peripheral oscillators. DMI, an antidepressant which increases the availability of norepinephrine (NE) in the synaptic cleft [98], appeared to be a good candidate to counteract the Dex-induced behavioural effects because it addresses most alterations we have documented: NE has been shown to upregulate AVP expression in the SCN [99–101], while DMI potentiates GR-mediated signalling [90,102]. Indeed, DMI treatment of Dex-males not only upregulated AVP expression in the SCN, but also upregulated hippocampal GR expression, in agreement with earlier reports [103–105]. Reinforcing the negative feedback loop regulating the HPA-axis activity presumably stabilizes intrinsic rhythmicity and reinforces circadian entrainment, thereby delaying the re-entrainment of spontaneous activity. This effect was strong enough to induce persistent changes in peripheral oscillators, as illustrated by the increase in amplitude of oscillations in clock gene expression in primary skin fibroblasts. Moreover, it appears that DMI treatment for about 5-6 weeks around the age of 6 months prevents the onset of Dex-induced depression-like phenotype at the age of 12 months. The restoration of circadian entrainment has been suggested to underlie the effects of specific anti-depressants such as ketamine [106,107] and agomelatine [108]. We can therefore speculate that DMI restored circadian entrainment for long enough to prevent Dex-induced alterations in hippocampal neurogenesis and the onset of depression-like behaviour.

In females, we found constitutive hyperactivity even in a familiar environment (the home cage at baseline), which is considered a core feature for ADHD animal models [109]. In female mice, hyperactivity has been described in DAT knockout models and DA receptor subtypes knockout models [110–112]. Dopaminergic input to the SCN from the VTA is a critical determinant of photic re-entrainment of spontaneous behaviour [111,113]. Decreased dopaminergic signalling was one of the pathways identified by SPIA analysis on bulk RNA-sequencing of SCN samples. Subsequent gene expression analyses suggest that decreased dopaminergic signalling is a global effect of prenatal exposure to Dex in females, which may provide a mechanistic explanation for both alterations of circadian re-entrainment and constitutive hyperactivity. Relevant to the phenotype found in Dex-females is the upregulation of *Gsk3b* expression in both the SCN and the hippocampus. Gsk3b destabilizes the molecular clock [114], and increased Gsk3b activity has been described in several psychiatric disorders, including bipolar disorder, schizophrenia, ADHD and depression [115]. This is in line with the circadian alterations described in ADHD patients, where bright light therapy stabilises circadian rhythms and reduces the intensity of core symptoms [116,117].

Spontaneous activity is a measurable read-out with complex context-dependent regulation mechanisms. Recording activity in home cage environment is technically challenging but is a non-invasive method to monitor behaviour in ethologically relevant conditions over extended periods of time. We have implemented a multivariate approach highlighting changes in the organisation of behaviour which are not possible to detect by individual features. For instance, we found that the distinction between patterns of activity in light and dark is drastically reduced following the phase shift, a challenge otherwise considered "mild". A major advantage of our approach for the analysis of spontaneous behaviour is the translational potential: activity monitoring in human subjects by means of actigraphy yields an objective measurement to support analogous analyses and interpretations, as illustrated in the following work using data collected from human subjects.

4.2 HUMANS (PAPER III AND IV)

We performed studies in patients suffering from depression, focusing on possible correlations between activity patterns from actigraphy recordings and the severity of depression symptoms estimated using the interview-based Montgomery-Åsberg Rating Scale (MADRS). In addition, we explored the correlation between activity patterns and the response to iCBT as antidepressant treatment.

The MADRS scale, introduced in 1979 by Montgomery and Åsberg, is the most commonly used depression rating scale in Europe and the UK[27]. It is currently used in 2 versions – one for clinician assessment, and one for self-assessment. The former includes an additional item (clinician's assessment of the patient's general state), while the latter has been shown to be a robust and easily applicable tool in everyday practice. The studies included in this thesis are based on the self-assessment version (MADRS-S). The usefulness of MADRS as outcome variable for ML algorithms may be challenged simply because of shear diversity of combinations potentially underlying any single value. We ran a preliminary numeric analysis of MADRS and found that a 9-item score with 7 levels/item yields more than 40 million combinations for a range between 0 and 54. In addition, a total score of 24 (*i.e.*, moderate depression) can be generated by ~2.5 million independent combinations. However, these calculations assume that the source of a MADRS score is a random number generator, and this assumption is not valid in real life. To start with, the range of MADRS is restricted by the inclusion/exclusion criteria set a priori for each clinical trial. Wild variations between individual item scores are unlikely because it is unreasonable to validate a MADRS score where, for instance, the subject reported high score for suicidal ideation (item 9), but very low score for pessimism (item 8). Efforts are underway to improve the reliability of data in clinical trials by establishing a consensus for flags and outlier identification [118,119]. Indirect support comes from recent analyses of PHQ-9 questionnaires (9-item, 4 levels/item; range 0-27; 262 434 possible combinations) in primary care settings identified a limited number of profiles based on individual items (14 or 20 individual profiles in ~10 000 records), suggesting that the number of combinations generated by interviewing subjects is considerably lower than expected from numeric analyses [120,121]. Lastly, the utility of

MADRS-S has been evaluated in detail, and the total score (*i.e.*, without consideration of underlying individual item scores) has been shown to be a reliable measure of symptom severity [122]. Next, we sought to define accuracy limits for modelling the MADRS score. We first considered the inter-rater and test-retest reliability for MADRS recording. Earlier reports estimate 95% CI = 7 face-to-face vs. telephone interviews [123] and up to 2.75 units difference across testing occasions [124], which suggests that the precision of estimation of MADRS for a subject lies within ±3 units. Next, we ran a numeric simulation considering variations of ±1 for each item and found that a range of ±3 units would include ~70% of possibilities. Lastly, we considered the minimum clinically important difference for response to treatment of 2 units on the MADRS scale [85]. In other words, the accuracy of the predicted score should be within 2 points in order to accommodate for errors in initial estimation, but not to obscure clinically relevant effects of antidepressant treatments.

The effects of antidepressant treatment can be estimated using the MADRS scores before and after treatment. A recent study has shown that a decrease of 10 units in MADRS score on average corresponds to a significant clinical improvement [125]. We calculated the response to treatment as relative difference from baseline (*i.e.*, difference between the MADRS score at the end of iCBT and the MADRS score before treatment, normalized to the MADRS score before treatment). This definition of response to treatment can be used on any symptom severity scale and has been used to stratify the patients into "non-responders" (less than 25% improvement), "partial responders" (between 25% and 49% improvement), and "responders" (> 50% improvement). We used the response to treatment as continuous output variable, despite theoretical hard bounds (improvement cannot exceed 100%). In real-life datasets, high positive values are not commonly encountered: dramatic worsening of symptoms under antidepressant treatment are limited, primarily because of ethical consideration embedded in the study design. Similarly, total disappearance of depression symptoms (MADRSpost = 0, *i.e.*, -100% response) is desirable and is often achieved but was not encountered in our study population. In this context we assumed a linear relationship between individual features and response to treatment in a range between -100% and 0%. While essentially discrete, since it is generated by combinations of integers, the relative change from baseline is better suited for regression models because it can assume considerably higher number of unique values than absolute difference (possible values: 1 800 *vs.* 108 for absolute difference; when the matrix is restricted according to the criteria specified in the study design, the number of unique values drops to 650 *vs.* 59). Exponential decay models have been suggested to better approximate the dynamics of response to treatment [126], but the change in MADRS over time was linear in the population included in this study (see [70]). In addition, we estimated the response to treatment using two values (before and after treatment), ignoring all intermediate datapoints. This is suitable for study designs with fixed follow-up intervals, as in the case of CBT, where the treatment is delivered in 10 weekly sessions.

4.2.1 Activity patterns and symptom severity

We took advantage of available actigraphy recordings from two independent populations, which allowed training an ensemble of models on one population and test its performance on the other. This approach allows reaching proof-of-concept for the pipeline and provides an indication of expectable attrition rate in ensemble size when pruning the original ensemble based on the performance on an independent dataset. In addition, one can get an indication of the most relevant features for modelling symptom severity, which may support the biological relevance of the alterations in activity patterns in relation to the severity of symptoms.

We found significant correlations with symptom severity in a limited number of features, namely negative correlation for the scaling exponent (alpha full; range 4 min – 24 h), and positive correlation for intradaily variability (IV5, IV30). We generated 14 892 models, whereof 3 837 survived filtering for internal validation. Surviving models had an average RMSE and R-squared of 1.84 ± 0.35 and 0.67 ± 0.11, respectively. Individual predictors vary greatly in the frequency of occurrence in models developed by brute force across levels of complexity. However, scaling coefficients and IV display consistent occurrence frequencies across models of increasing complexity.

For internal validation of our models, we used a heuristic approach considering the required accuracy of MADRS estimation. To measure the accuracy of our models, we applied RMSE since it penalizes all deviations and is sensitive to outliers. In our datasets restricting to RMSE <3 yielded an average accuracy of 2.7, and an absolute error below 3 in 75% of the cases. We evaluated the performance of the surviving models on an independent population and applied the same validation criteria, which further reduced the number of validated models to 192. The average RMSE and R-squared in models surviving external validation were 2.70 ± 0.24 and 0.59 ± 0.09 respectively. We analysed the standardized coefficients for the 192 models surviving external validation which revealed strong consistency across models for most independent predictors. On average alpha full, IS5 and RA were all included on average in > 50% of the models in descending order, with alpha full included in > 75% of the models.

The brute force approach trains individual models without prior information from earlier generated models to increase accuracy in subsequent steps. We, therefore, used stepwise machine learning (ML) algorithms to train models of increasing complexity. ML yielded 18 models which like the brute force models, underwent internal and external validation. Of the 18 models generated, 14 survived internal validation, and 5 survived external validation (Pearson R > 0.576, RMSE < 3). We calculated the proportion of absolute residuals below 1 to 5 MADRS units in 1-unit increments and found that 54% of the cases were within 2 units, 75% within 3 units, and 87% within 4 units of the observed scores. The distribution of estimation errors for trained with a forward stepwise procedure was similar in outcome to the models discovered by brute force: alpha full, IS5, IS30, and RA were among the most common features in the models surviving external validation.

4.2.2 Molecular clock function

Accumulating evidence points to the uncoupling of oscillations in clock gene expression from the light/dark cycle to be a feature of depression. Clock gene expression in post-mortem material collected from depressed patients is characterized by reduced amplitude and desynchronization from the light/dark cycle [127]. We found a similar pattern in our experimental model, where peripheral oscillators are uncoupled from the central clock in Dex-males before the onset of depression-like behaviour. In MDD patients we observed sparse correlations between oscillations in clock gene expression and features of activity patterns, which did not match findings in HCs. Thus, we found a significantly lower angle of entrainment (*i.e.*, constitutive gene expression resumes later after repressing it through the synchronization procedure) for *BMAL1* expression, which was associated with lower day-to-day variability (ddv). This suggests that weaker drive by the internal clock allows for stronger coupling with external entrainers. This interpretation is supported by the association of lower angle of entrainment for *BMAL1* expression with lower fragmentation (IV5, IV30 and IV60) and higher scaling exponent in HCs, which point to consolidation of rest and activity bouts favouring oscillation with longer period (*e.g.*, circadian).

4.2.3 Activity patterns and the response to antidepressant treatment

The investigation of response to treatment took advantage of available recordings from HCs matched for age, sex, and intellectual ability. We explored first the differences between MDD patients and HCs; second, we examined the changes in relation to the magnitude of antidepressant response to iCBT; lastly, we explored the correlations between circadian rhythms and activity patterns and the magnitude of antidepressant response to iCBT. Given the limited number of recordings available, the purpose of this study was to develop a pipeline for model training and analysis of linear models using the systematic ensemble development approach.

We started by analysing the activity profile of HCs and patients diagnosed with depression. Average motion PDFs profiles suggest that MDD patients display a flatter average circadian profile, and a more abrupt onset of activity, which were not accounted for by shifted circadian profile in MDD patients as compared to HCs. Following iCBT, the average circadian profile displayed 3 well-defined peaks, but the abrupt onset of circadian profile was preserved. We then investigated whether there were any qualitative differences in the underlying time series using individual features. We found only scattered differences between HCs and MDDpre (MDD patients before treatment), and MDDpost (MDD patients after treatment), which did not survive correction for multiple comparisons. However, when we analysed the correlation between individual features, we found different patterns in MDDpre compared to HCs. In MDDpre, age displays a negative correlation with the location of the circadian peak, suggesting older patients experience earlier occurrence of the circadian peak of activity. In contrast, we observed positive correlation between age and intradaily variability (IV), and negative correlation between age and scaling exponent (alpha full), indicating a gradual decrease in structured patterns of activity with ageing. Such differences may be generated by

alterations in molecular clock function. We analysed the expression of core clock genes *BMAL1* and *PER2* in primary fibroblasts cultures derived from skin samples collected from the patients included in the study. The function of the molecular clock was correlated with features of circadian activity, where we focused on amplitude and angle of entrainment as core features of circadian entrainment. MDDpre had sparse and weak correlations between oscillations in clock gene expression and features of activity patterns. The higher amplitude of *BMAL1* was associated with a longer circadian period and a higher angle of entrainment with higher ddv. For *PER2*, the higher amplitude was associated with higher IS and a higher angle of entrainment with a shorter circadian period. Furthermore, for *PER2*, a higher relative angle of entrainment was associated with a lower scaling exponent. HCs had a higher number of significant correlations than observed in MDD patients.

To explore the potential multivariate correlations between activity patterns before treatment and the magnitude of response to iCBT as antidepressant treatment, we generated two separate ensembles of linear regression models which included either actigraphy alone or together with clock gene expression in skin fibroblasts. The accuracy of the ensemble including clock gene expression data was marginally better than actigraphy alone and was based on a considerably higher number of independent models. To test the likelihood of getting results by chance, we followed an empirical approach, namely repeating the ensemble training procedure after randomly shuffling the outcome variable. The size of the ensemble remaining after pruning (using the criteria listed above) was used for evaluating the likelihood of generating similar results by chance. The distribution of number of validated models (373 iterations) followed a Pareto distribution, which yielded an estimated likelihood of occurrence by chance of ~0.006.

Next, we sought to identify the most relevant features for fitting the response to iCBT. To this end we calculated the coefficient of variation (CV) for individual features across models. We found rather stable CV for individual features, and we used an arbitrary threshold of 0.5 to stratify them into 2 groups. The features found in the group with CV below 0.5 overlap to a large extent between the two ensembles and do not include features related to clock gene expression. The analysis of coefficients suggests that larger improvements in MADRS score are associated with increased age, lower IV60, lower IS30 and IS60, more robust circadian rhythms (higher RA and M10, lower L5, and earlier circadian trough of activity, L5L) and higher day-to-day variability (higher ddv, rmssd, rmsmd).

Finally, we investigated whether we could identify significant correlations between the magnitude of change in individual features and the response to treatment. For this experiment we had only 8 pairs actigraphy recordings available. First, we analysed the changes in circadian profile and found that larger improvement following iCBT, is associated with an increase in activity immediately before noon and mid-afternoon, as well as a decrease in activity around 9 in the evening. This was corroborated by the changes in the feature space, where we found larger improvements in response to iCBT to correlate with a shift towards earlier occurrence of the circadian peak of activity and a decrease in ddv.

4.2.4 General discussion and limitations

Activity and depression are intrinsically linked, as psychomotor retardation and alterations in sleep are core symptoms of depression, and physical activity as an anti-depressant treatment may reduce depressive symptoms [128,129]. Furthermore, depression symptom severity and levels of activity are connected so that on average higher severity correlates with lower levels of activity, particularly in moderate activity band [130]. From a technology perspective, actigraphy is a relatively low-cost and non-invasive method to collect longitudinal data in human subjects. It essentially offers an insight into modulation of activity over extended periods of time, in the context of multiple circadian entrainers ranging from internal drive, 24-h light-dark cycle, and social entrainers. In our case, it allows the translation of information obtained from animal models to patterns of activity in human subjects. The analysis of the circadian profile of activity is an easy-to-implement approach to evaluate circadian disruption. In our study, we used a recently developed non-parametric method [73], which offers an intuitive geometric interpretation for complex underlying mathematical concepts. The use of motion probability density function to construct the circadian profile cancels the noise induced by variations in the total amount of activity recorded on different days and thereby reveals a simplified pattern which can be readily compared between groups. In MDD patients, we found that changes in circadian profile, which correlate with the magnitude of response to iCBT occur in regions that are not initially different from HCs. This indicates that the circadian profile of MDD patients does not "normalise" in the patients that respond to treatment. We also observed that larger improvement is associated with a shift in the location of the circadian peak of activity towards earlier clock time.

The development of model ensembles and aggregation of output has the advantage of enhancing the generalizability of findings based on relatively small samples [131]. Training model ensembles, however, does not grant improvement in prediction accuracy as compared to individual models. In our hands, the aggregated output outperformed individual models by a factor of 2 to 4 for both symptom severity and response to treatment. The accuracy of aggregated output indicates that the ensemble including clock gene expression data performs marginally better than the ensemble based exclusively on actigraphy features. This suggests that in a clinical setting, actigraphy alone would be sufficient for modelling the response to iCBT. Thus, we bring proof of concept evidence for correlations between individual patterns of activity and depression symptom severity, as well as for the response to iCBT as

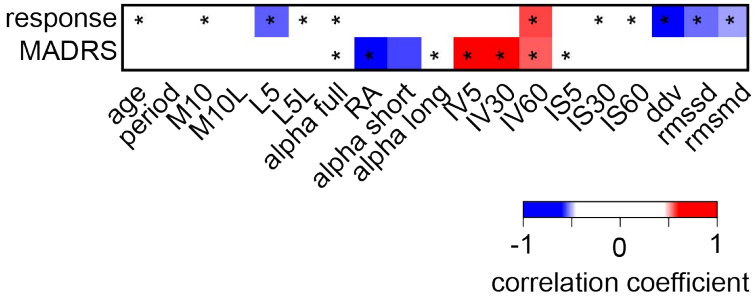

Figure 4-6 Correlation between individual features and total MADRS score or response to iCBT. Asterisks depict features identified as most relevant by coefficient analysis. Note the very small overlap between the two subsets of features.

antidepressant treatment. We further analysed the performance of individual features in each ensemble. Of note, there is very little overlap between the sets of features identified as most relevant for either model ensemble (see Fig. 4-6) The most relevant features for modelling symptom severity included the complexity of activity patterns (scaling exponent), the strength of coupling between circadian entrainers (IS) and the robustness of circadian rhythms (RA). The analysis of coefficients indicates that more severe symptoms are associated with less complex patterns of activity, stronger coupling of activity with circadian entrainers, and less robust circadian rhythms. In other words, more severe symptoms are associated with a decreased internal drive to steer one's activity in a circadian context, and instead passively follow circadian entrainers. In contrast, the response to iCBT is best modelled by age, robustness of circadian rhythms (RA), variability between days (ddv) and within (IV60) days, and intradaily stability (IS30, IS60) before treatment. The analysis of coefficients suggests that a larger improvement is associated with less fragmented activity, more robust circadian rhythms, looser circadian entrainment, and higher day-to-day variability before treatment. This is consistent with a strong internal drive which is overriding or otherwise escaping circadian entrainment by environmental stimuli. Following iCBT, we found a significant association of larger improvement with a decrease in day-to-day variability, which may be accounted for by stronger coupling to environmental clues.

Limitations of the studies

The approach based on ensemble training increases the generalizability of the findings because individual models may favour different subsets in the training dataset, and the aggregated fitting is less sensitive to outliers. However, our study is based on a small population, which implies a high risk of overfitting. Ideally, the ensemble training should be based on a large dataset where inclusion criteria are not very restrictive, and the performance should be tested on several independent datasets. Here we focused on developing a sound pipeline for data processing and feature extraction for actigraphy as objective measurement during a depressive episode. In Paper III the training dataset was collected from patients recruited for a clinical trial assessing the response to iCBT, which may include more variable symptom profiles and pathological mechanisms. In contrast, the test dataset was acquired from patients included in the study only if they did not respond to SSRI drugs and would be eligible for ketamine treatment – hence a strong selection bias is expected. The fact that models trained on an intrinsically more variable population sample perform very well on the more strictly selected population support the applicability of our approach. Nevertheless, there is a risk of overfitting the available pair of datasets, and the outcome of external validation can be assumed to be rather restrictive.

All patients included in this study were diagnosed with a unipolar major depressive episode, and the model was trained to predict the MADRS score registered prior to the actigraphy recording, under the implicit assumption that activity was recorded in a stable state (*i.e.*, no significant variations in symptom severity expected during recording time). In contrast, skin samples were collected from patients at a later timepoint. We assumed that primary fibroblast

cultures offer an insight into the function of the molecular clock and may therefore reveal alterations relevant for the propensity to develop depressive episodes rather than for the ongoing depressive episode. The assumption is based on previous studies showing that the molecular clock in primary cultures of skin fibroblasts maintains in culture (*ex vivo*) characteristic features of circadian clocks *in vivo* (*e.g.*, internal period, robustness of circadian oscillations in clock gene expression) [131–133]. In addition, core clock gene variants are associated with depressive disorders or depression vulnerability [56,134]. In this context, the timing of collecting skin samples for derivation of primary cultures of fibroblasts is probably not relevant. The analysis of clock gene expression may be relevant for differentiating between MDD patients and HCs, but it appears to have only limited contribution to model the response to iCBT as antidepressant treatment.

In Paper III, ongoing antidepressant treatment was an exclusion criterion for the training population, and the actigraphy was recorded after a reasonable washout period in the test population. The impact of psychoactive drugs (acting on neurotransmitter systems which regulate circadian activity, *e.g.*, glutamate, serotonin, noradrenaline, acetylcholine; reviewed in ref. [134]) on activity patterns of psychiatric patients is not fully understood [56]. Therefore, potential correlations between patterns of activity and symptom severity in patients undergoing antidepressant treatment cannot be extrapolated from our data and require a separate investigation.

From a clinical application perspective, our results indicate that actigraphy could be a useful tool in the individual evaluation of patients suffering from depression. Here we developed a pipeline which is limited by the number of participants and larger confirmatory studies are required before clinical implementation.

5 CONCLUDING REMARKS

The nervous system is highly susceptible to challenges during development, and disruption of normal development can have long-term consequences, potentially leading to adult-onset diseases. Maternal stress, exposure to neurotoxic compounds, and inflammation are among the factors which can affect the developing nervous system. The general aim of this thesis was to investigate the consequences of prenatal exposure to GC using mouse *in utero* exposed to Dex during the last week of gestation. The long-term effects of prenatal exposure to Dex were different in male and female offspring, suggesting sex-specific underlying mechanisms. Males developed late-onset depression-like behaviour, which was prevented by treatment with DMI at 6 months of age. In contrast, females were hyperactive in the familiar environment –a phenotype resembling ADHD. The investigation of behavioural alterations in females revealed an unexpected obstacle: females are grossly underrepresented in neuroscience research, and we were largely unable to find previous reports to compare our results with. Given the difference in response to exposures, our results emphasise the need for inclusion of both sexes in experimental and medical research in general.

We used a system to monitor locomotor activity of group-housed animals which allowed simultaneous observation of all individuals in the cage over extended periods of time. In preparation for data analysis, we paid special attention to natural rodent behaviour, which could be measured using our system, such as impact of social environment and uneven spatial distribution of specific behaviours (*e.g.*, nest area). Next, we implemented an approach based on algorithms initially developed for analysis of RNA sequencing data, which allowed the quantification of changes in behaviour patterns impossible to differentiate at individual feature level.

Investigations in human subjects inevitably carry more noise than experimental research in controlled laboratory conditions. Experimental models, however, may be fraught with artefacts because of the artificial setup, yielding results of questionable reproducibility. Therefore, the ability to evaluate animal behaviour under minimally invasive conditions, albeit more complex, has open a door into better understanding of complex animal behaviours. We have developed a pipeline to explore the correlations between patterns of activity and symptom severity or response to iCBT as antidepressant treatment in MDD patients. Despite limitations due to population size, we addressed relevant questions linking the data-driven approach and biological interpretations of models. In addition, the minimal overlap between subsets of features modelling different outcomes (symptom severity and response to iCBT) suggests that the pipeline is robust and may be used for addressing additional questions, such as the response to specific antidepressant drugs.

Altogether, this thesis is based on a research journey from rodents to human and highlights the relevance of experimental research to get insight in human behaviour in health and disease.

6 ACKNOWLEDGEMENTS

This work was funded by Swedish research Council (VR), The Brain Foundation (Hjärnfonden), Karolinska Institutet Funds for Doctoral Education (KID), Torsten Söderberg Foundation. We would like to thank Philips for supplying hardware and support for recording actigraphy.

This project would have gone nowhere, if it was not for the collaborations, guidance and support I have received throughout the 4-year period. I would like to thank the following:

Sandra Ceccatelli, my supervisor, first for your daring experiment of hiring an engineer as a Ph.D. student. Your exceptional scientific expertise has been a great inspiration, and your high expectations have been a challenge that allowed me to grow not only as a scientist, but as a person.

Stefan Spulber, my co-supervisor, it has been a privilege to work with you. If there is such a thing as "knowing too much" then it describes you. You have taught me new techniques, perspectives, and scientific approaches on every occasion, and I think I have barely scratched the surface. While my Ph.D. days are over, we will hopefully collaborate in some shape or form in the future.

Johan Lundberg, my co-supervisor, for your unique clinical perspective and help with framing our research into a clinical setting.

Lua Reis, for your positive attitude, taking care of all the cell work and the fascinating introduction to "Brazilian" time management.

Raj Bose, for your insights and help with the final experiments for paper II when I was away from the lab.

Dasiel Oscar Borotto-Escuella, for your extensive technical expertise of the PLA and confocal microscope and talks over coffee.

Dagmar Galter, for your help with experimental setup and your support during this project has been a big help.

Zongli Zheng, Jan Keung, Virpi Ahola (Ming Wai Lau Centre), my collaborators in Hong Kong. While my visit was cut short, you made me feel very welcome and I am grateful for our collaboration could continue despite the setbacks.

Sylwia Owczarek Jacobsen, my mentor, providing well needed sanity checks throughout the project.

Lara Friess, the punctual German who would complain whenever I was 5 min late for the pub. It has been wonderful to have you through this Ph.D. "adventure" and to share our successes and setbacks, so many setbacks.

Annika Andersson, you were a late asset in Biomedicum, but a most welcome one. Finally, someone to discuss weight training, protein powder and exercises with. May we grow ever stronger!

Family & Friends, for the love and support during this 4-year period, and all the weekend visits that got me a bit more outside of the house that I would have liked, but which I definitely needed.

Kathrine, it was surprisingly easy to convince you to come to Stockholm with me for this project. Your support has been invaluable especially after Johannes entered our lives, and I will miss our Swedish solitude and our endless visits to the bakery. I would have managed to make it alone during this project, but it wouldn't have half as fun without you.

Johannes, my boy, someone once said: "a child will destroy your life, but replace it with a better one", you most certainly have.

7 REFERENCES

1. Gillman MW. Developmental origins of health and disease. *N Engl J Med*. 2005;353(17):1848-1850. doi:10.1056/NEJMe058187

2. Cao-Lei L, de Rooij SRR, King S, et al. Prenatal stress and epigenetics. *Neurosci Biobehav Rev*. 2020;117(November 2016):198-210. doi:10.1016/j.neubiorev.2017.05.016

3. Oster H, Damerow S, Kiessling S, et al. The circadian rhythm of glucocorticoids is regulated by a gating mechanism residing in the adrenal cortical clock. *Cell Metab*. 2006;4(2):163-173. doi:10.1016/j.cmet.2006.07.002

4. Sheng JA, Bales NJ, Myers SA, et al. The Hypothalamic-Pituitary-Adrenal Axis: Development, Programming Actions of Hormones, and Maternal-Fetal Interactions. *Front Behav Neurosci*. 2021;14. doi:10.3389/fnbeh.2020.601939

5. Mastorakos G, Ilias I. Maternal and fetal hypothalamic-pituitary-adrenal axes during pregnancy and postpartum. *Ann N Y Acad Sci*. 2003;997(1):136-149. doi:10.1196/annals.1290.016

6. Kadmiel M, Cidlowski JA. Glucocorticoid receptor signaling in health and disease. *Trends Pharmacol Sci*. 2013;34(9):518-530. doi:10.1016/j.tips.2013.07.003

7. Panettieri RA, Schaafsma D, Amrani Y, Koziol-White C, Ostrom R, Tliba O. Non-genomic Effects of Glucocorticoids: An Updated View. *Trends Pharmacol Sci*. 2019;40(1):38-49. doi:10.1016/j.tips.2018.11.002

8. Cameron HA, Gould E. Adult neurogenesis is regulated by adrenal steroids in the dentate gyrus. *Neuroscience*. 1994;61(2):203-209. doi:10.1016/0306-4522(94)90224-0

9. Meyer JS. Early adrenalectomy stimulates subsequent growth and development of the rat brain. *Exp Neurol*. 1983;82(2):432-446. doi:10.1016/0014-4886(83)90415-6

10. Yehuda R, Fairman KR, Meyer JS. Enhanced Brain Cell Proliferation Following Early Adrenalectomy in Rats. *J Neurochem*. 1989;53(1):241-248. doi:10.1111/j.1471-4159.1989.tb07320.x

11. Harris A, Seckl J. Glucocorticoids, prenatal stress and the programming of disease. *Horm Behav*. 2011;59(3):279-289. doi:10.1016/j.yhbeh.2010.06.007

12. Khulan B, Drake AJ. Glucocorticoids as mediators of developmental programming effects. *Best Pract Res Clin Endocrinol Metab*. 2012;26(5):689-700. doi:10.1016/j.beem.2012.03.007

13. Ward IL. The prenatal stress syndrome: Current status. *Psychoneuroendocrinology*. 1984;9(1):3-11. doi:10.1016/0306-4530(84)90016-7

14. Liggins GC, Howie RN. A controlled trial of antepartum glucocorticoid treatment for prevention of the respiratory distress syndrome in premature infants. *Pediatrics*. 1972;50(4):515-525. http://www.ncbi.nlm.nih.gov/pubmed/4561295.

15. Waffarn F, Davis EP. Effects of antenatal corticosteroids on the hypothalamic-pituitary-adrenocortical axis of the fetus and newborn: experimental findings and clinical considerations. *Am J Obstet Gynecol*. 2012;207(6):446-454. doi:10.1016/j.ajog.2012.06.012

16. Levitt NS, Lindsay RS, Holmes MC, Seckl JR. Dexamethasone in the Last Week of Pregnancy Attenuates Hippocampal Glucocorticoid Receptor Gene Expression and Elevates Blood Pressure in the Adult Offspring in the Rat. *Neuroendocrinology*. 1996;64(6):412-418. doi:10.1159/000127146

17. Sloboda DM, Moss TJMM, Li S, et al. Prenatal betamethasone exposure results in pituitary-adrenal hyporesponsiveness in adult sheep. *Am J Physiol Metab*. 2007;292(1):E61-E70. doi:10.1152/ajpendo.00270.2006

18. Ahlbom E, Gogvadze V, Chen M, Celsi G, Ceccatelli S. Prenatal exposure to high levels of glucocorticoids increases the susceptibility of cerebellar granule cells to oxidative stress-induced cell death. *Proc Natl Acad Sci*. 2000;97(26):14726-14730. doi:10.1073/pnas.260501697

19. Drake AJ, Liu L, Kerrigan D, Meehan RR, Seckl JR. Multigenerational programming in the glucocorticoid programmed rat is associated with generation-specific and parent of origin effects. *Epigenetics*. 2011;6(11):1334-1343. doi:10.4161/epi.6.11.17942

20. Drake AJ, Walker BR, Seckl JR. Intergenerational consequences of fetal programming by in utero exposure to glucocorticoids in rats. *Am J Physiol Integr Comp Physiol*. 2005;288(1):R34-R38. doi:10.1152/ajpregu.00106.2004

21. Bhutta AT, Cleves MA, Casey PH, Cradock MM, Anand KJS. Cognitive and behavioral outcomes of school-aged children who were born preterm: A meta-analysis. *J Am Med Assoc*. 2002;288(6):728-737. doi:10.1001/jama.288.6.728

22. Strang-Karlsson S, Räikkönen K, Pesonen A-K, et al. Very Low Birth Weight and Behavioral Symptoms of Attention Deficit Hyperactivity Disorder in Young Adulthood: The Helsinki Study of Very-Low-Birth-Weight Adults. *Am J Psychiatry*. 2008;165(10):1345-1353. doi:10.1176/appi.ajp.2008.08010085

23. Abel KM, Wicks S, Susser ES, et al. Birth weight, schizophrenia, and adult mental disorder: is risk confined to the smallest babies? *Arch Gen Psychiatry*. 2010;67(9):923-930. doi:10.1001/archgenpsychiatry.2010.100

24. Thompson C, Syddall H, Rodin I, Osmond C, Barker DJPP. Birth weight and the risk of depressive disorder in late life. *Br J Psychiatry*. 2001;179(5):450-455. doi:10.1192/bjp.179.5.450

25. Alati R, Lawlor DA, Mamun A Al, et al. Is there a fetal origin of depression? Evidence from the Mater University Study of Pregnancy and its outcomes. *Am J Epidemiol*. 2007;165(5):575-582.

26. Räikkönen K, Pesonen AK, Heinonen K, et al. Depression in young adults with very low birth weight: The Helsinki study of very low-birth-weight adults. *Arch Gen Psychiatry*. 2008;65(3):290-296. doi:10.1001/archgenpsychiatry.2007.40

27. Montgomery SM. Depressive symptoms in acute schizophrenia. *Prog Neuropsychopharmacol*. 1979;3(4):429-433. doi:10.1016/0364-7722(79)90058-4

28. Ferrari F, Villa RF. The Neurobiology of Depression: an Integrated Overview from Biological Theories to Clinical Evidence. *Mol Neurobiol*. 2017;54(7):4847-4865. doi:10.1007/s12035-016-0032-y

29. Antoniuk S, Bijata M, Ponimaskin E, Wlodarczyk J. Chronic unpredictable mild stress for modeling depression in rodents: Meta-analysis of model reliability. *Neurosci*

Biobehav Rev. 2019;99(December 2018):101-116. doi:10.1016/j.neubiorev.2018.12.002

30. Ding Y, Dai J. Advance in Stress for Depressive Disorder. In: *Advances in Experimental Medicine and Biology*. Vol 1180. ; 2019:147-178. doi:10.1007/978-981-32-9271-0_8

31. Powers SI, Laurent HK, Gunlicks-Stoessel M, Balaban S, Bent E. Depression and anxiety predict sex-specific cortisol responses to interpersonal stress. *Psychoneuroendocrinology*. 2016;69:172-179. doi:10.1016/j.psyneuen.2016.04.007

32. Slavich GM, Sacher J. Stress, sex hormones, inflammation, and major depressive disorder: Extending Social Signal Transduction Theory of Depression to account for sex differences in mood disorders. *Psychopharmacology (Berl)*. 2019;236(10):3063-3079. doi:10.1007/s00213-019-05326-9

33. Spulber S, Conti M, DuPont C, et al. Alterations in circadian entrainment precede the onset of depression-like behavior that does not respond to fluoxetine. *Transl Psychiatry*. 2015;5(7):e603-e603. doi:10.1038/tp.2015.94

34. Grissom NM, Reyes TM. Gestational overgrowth and undergrowth affect neurodevelopment: similarities and differences from behavior to epigenetics. *Int J Dev Neurosci*. 2013;31(6):406-414. doi:10.1016/j.ijdevneu.2012.11.006

35. Longo S, Bollani L, Decembrino L, Di Comite A, Angelini M, Stronati M. Short-term and long-term sequelae in intrauterine growth retardation (IUGR). *J Matern Neonatal Med*. 2013;26(3):222-225. doi:10.3109/14767058.2012.715006

36. Pesonen AK, Räikkönen K, Lano A, Peltoniemi O, Hallman M, Kari MA. Antenatal betamethasone and fetal growth in prematurely born children: Implications for temperament traits at the age of 2 years. *Pediatrics*. 2009;123(1):e31-e37. doi:10.1542/peds.2008-1809

37. Cole J, Costafreda SG, McGuffin P, Fu CHY. Hippocampal atrophy in first episode depression: A meta-analysis of magnetic resonance imaging studies. *J Affect Disord*. 2011;134(1-3):483-487. doi:10.1016/j.jad.2011.05.057

38. Masi G, Brovedani P. The hippocampus, neurotrophic factors and depression: Possible implications for the pharmacotherapy of depression. *CNS Drugs*. 2011;25(11):913-931. doi:10.2165/11595900-000000000-00000

39. Moncrieff J, Cooper RE, Stockmann T, Amendola S, Hengartner MP, Horowitz MA. The serotonin theory of depression: a systematic umbrella review of the evidence. *Mol Psychiatry*. July 2022. doi:10.1038/s41380-022-01661-0

40. Stone MB, Yaseen ZS, Miller BJ, Richardville K, Kalaria SN, Kirsch I. Response to acute monotherapy for major depressive disorder in randomized, placebo controlled trials submitted to the US Food and Drug Administration: individual participant data analysis. *BMJ*. 2022;378:e067606. doi:10.1136/bmj-2021-067606

41. Bhadra U, Thakkar N, Das P, Pal Bhadra M. Evolution of circadian rhythms: from bacteria to human. *Sleep Med*. 2017;35:49-61. doi:10.1016/j.sleep.2017.04.008

42. Mure LS, Le HD, Benegiamo G, et al. Diurnal transcriptome atlas of a primate across major neural and peripheral tissues. *Science*. 2018;359(6381):eaao0318. doi:10.1126/science.aao0318

43. Albrecht U. Timing to Perfection: The Biology of Central and Peripheral Circadian Clocks. *Neuron*. 2012;74(2):246-260. doi:10.1016/j.neuron.2012.04.006

44. Balsalobre A, Brown SA, Marcacci L, et al. Resetting of Circadian Time in Peripheral Tissues by Glucocorticoid Signaling. *Science*. 2000;289(5488):2344-2347. doi:10.1126/science.289.5488.2344

45. Buhr ED, Takahashi JS. Molecular Components of the Mammalian Circadian Clock. In: *Handbook of Experimental Pharmacology*. ; 2013:3-27. doi:10.1007/978-3-642-25950-0_1

46. Dashti HS, Redline S, Saxena R. Polygenic risk score identifies associations between sleep duration and diseases determined from an electronic medical record biobank. *Sleep*. 2019;42(3). doi:10.1093/sleep/zsy247

47. Fleming J. Sleep architecture changes in depression: Interesting finding or clinically useful. *Prog Neuro-Psychopharmacology Biol Psychiatry*. 1989;13(3-4):419-429. doi:10.1016/0278-5846(89)90130-9

48. Wyse CA, Celis Morales CA, Graham N, et al. Adverse metabolic and mental health outcomes associated with shiftwork in a population-based study of 277,168 workers in UK biobank. *Ann Med*. 2017;49(5):411-420. doi:10.1080/07853890.2017.1292045

49. Mendoza J. Circadian insights into the biology of depression: Symptoms, treatments and animal models. *Behav Brain Res*. 2019;376:112186. doi:10.1016/j.bbr.2019.112186

50. Emens J, Lewy A, Kinzie JM, Arntz D, Rough J. Circadian misalignment in major depressive disorder. *Psychiatry Res*. 2009;168(3):259-261. doi:10.1016/j.psychres.2009.04.009

51. Humpston C, Benedetti F, Serfaty M, et al. Chronotherapy for the rapid treatment of depression: A meta-analysis. *J Affect Disord*. 2020;261(April 2019):91-102. doi:10.1016/j.jad.2019.09.078

52. Silva S, Bicker J, Falcão A, Fortuna A. Antidepressants and Circadian Rhythm: Exploring Their Bidirectional Interaction for the Treatment of Depression. *Pharmaceutics*. 2021;13(11). doi:10.3390/pharmaceutics13111975

53. Lavebratt C, Sjöholm LK, Partonen T, Schalling M, Forsell Y. PER2 variantion is associated with depression vulnerability. *Am J Med Genet Part B Neuropsychiatr Genet*. 2010;153B(2):570-581. doi:10.1002/ajmg.b.31021

54. Lavebratt C, Sjöholm LK, Soronen P, et al. CRY2 Is Associated with Depression. Reif A, ed. *PLoS One*. 2010;5(2):e9407. doi:10.1371/journal.pone.0009407

55. Gyorik D, Eszlari N, Gal Z, et al. Every Night and Every Morn: Effect of Variation in CLOCK Gene on Depression Depends on Exposure to Early and Recent Stress. *Front Psychiatry*. 2021;12. doi:10.3389/fpsyt.2021.687487

56. Sjoholm LK, Kovanen L, Saarikoski ST, et al. CLOCK is suggested to associate with comorbid alcohol use and depressive disorders. *J Circadian Rhythms*. 2010;8:1. doi:10.1186/1740-3391-8-1

57. Partonen T, Treutlein J, Alpman A, et al. Three circadian clock genes Per2, Arntl, and Npas2 contribute to winter depression. *Ann Med*. 2007;39(3):229-238.

doi:10.1080/07853890701278795

58. Landgraf D, Long JE, Proulx CD, Barandas R, Malinow R, Welsh DK. Genetic Disruption of Circadian Rhythms in the Suprachiasmatic Nucleus Causes Helplessness, Behavioral Despair, and Anxiety-like Behavior in Mice. *Biol Psychiatry*. 2016;80(11):827-835. doi:10.1016/j.biopsych.2016.03.1050

59. Ben-Hamo M, Larson TA, Duge LS, et al. Circadian Forced Desynchrony of the Master Clock Leads to Phenotypic Manifestation of Depression in Rats. *eneuro*. 2016;3(6):ENEURO.0237-16.2016. doi:10.1523/ENEURO.0237-16.2016

60. Vadnie CA, McClung CA. Circadian Rhythm Disturbances in Mood Disorders: Insights into the Role of the Suprachiasmatic Nucleus. *Neural Plast*. 2017;2017:1504507. doi:10.1155/2017/1504507

61. Lyall LM, Wyse CA, Graham N, et al. Association of disrupted circadian rhythmicity with mood disorders, subjective wellbeing, and cognitive function: a cross-sectional study of 91 105 participants from the UK Biobank. *The Lancet Psychiatry*. 2018;5(6):507-514. doi:10.1016/S2215-0366(18)30139-1

62. Bondopadhyay U, Diaz-Orueta U, Coogan AN. The Role of the Circadian System in Attention Deficit Hyperactivity Disorder. *Adv Exp Med Biol*. 2021;1344:113-127. doi:10.1007/978-3-030-81147-1_7

63. Antle MC, van Diepen HC, Deboer T, Pedram P, Pereira RR, Meijer JH. Methylphenidate Modifies the Motion of the Circadian Clock. *Neuropsychopharmacology*. 2012;37(11):2446-2455. doi:10.1038/npp.2012.103

64. Mamlouk GM, Dorris DM, Barrett LR, Meitzen J. Sex bias and omission in neuroscience research is influenced by research model and journal, but not reported NIH funding. *Front Neuroendocrinol*. 2020;57(December 2019):100835. doi:10.1016/j.yfrne.2020.100835

65. Riecher-Rössler A. Sex and gender differences in mental disorders. *The Lancet Psychiatry*. 2017;4(1):8-9. doi:10.1016/S2215-0366(16)30348-0

66. Conti M, Spulber S, Raciti M, Ceccatelli S. Depressive-like phenotype induced by prenatal dexamethasone in mice is reversed by desipramine. *Neuropharmacology*. 2017;126:242-249. doi:10.1016/j.neuropharm.2017.09.015

67. Blumberg MS, Seelke AMH, Lowen SB, Karlsson KÆ. Dynamics of sleep-wake cyclicity in developing rats. *Proc Natl Acad Sci*. 2005;102(41):14860-14864. doi:10.1073/pnas.0506340102

68. Frey BJ, Dueck D. Clustering by passing messages between data points. *Science*. 2007;315(5814):972-976. doi:10.1126/science.1136800

69. McInnes L, Healy J, Melville J. UMAP: Uniform Manifold Approximation and Projection for Dimension Reduction. *arXiv*. 2018. http://arxiv.org/abs/1802.03426.

70. Svensson JE, Svanborg C, Plavén-Sigray P, et al. Serotonin transporter availability increases in patients recovering from a depressive episode. *Transl Psychiatry*. 2021;11:264. doi:10.1038/s41398-021-01376-w

71. Ekholm B, Spulber S, Adler M. A randomized controlled study of weighted chain blankets for insomnia in psychiatric disorders. *J Clin Sleep Med*. 2020;16(9):1567-

1577. doi:10.5664/jcsm.8636

72. Tiger M, Veldman ER, Ekman C-J, Halldin C, Svenningsson P, Lundberg J. A randomized placebo-controlled PET study of ketamine´s effect on serotonin1B receptor binding in patients with SSRI-resistant depression. *Transl Psychiatry*. 2020;10(1):159. doi:10.1038/s41398-020-0844-4

73. Marín-Garciá A, Fossion R, Müller MF, Ríos-Herrera W, Rivera AL. A non-parametric model: Free analysis of actigraphic recordings of acute insomnia patients. *R Soc Open Sci*. 2022;9(2). doi:10.1098/rsos.210463

74. Gonçalves BSB, Adamowicz T, Louzada FM, Moreno CR, Araujo JF. A fresh look at the use of nonparametric analysis in actimetry. *Sleep Med Rev*. 2015;20:84-91. doi:10.1016/j.smrv.2014.06.002

75. Hu K, Ivanov PC, Chen Z, Hilton MF, Stanley HE, Shea SA. Non-random fluctuations and multi-scale dynamics regulation of human activity. *Neuroscience*. 2004;149(1-2):508-517. doi:10.1016/j.physa.2004.01.042.Non-random

76. Gonçalves BSB, Cavalcanti PPRA, Tavares GR, Campos TF, Araujo JF. Nonparametric methods in actigraphy: An update. *Sleep Sci*. 2014;7(3):158-164. doi:10.1016/j.slsci.2014.09.013

77. Saragiotis C. Lomb normalized periodogram. 2021. https://se.mathworks.com/matlabcentral/fileexchange/22215-lomb-normalized-periodogram.

78. Sokolove PG, Bushell WN. The chi square periodogram: Its utility for analysis of circadian rhythms. *J Theor Biol*. 1978;72(1):131-160. doi:10.1016/0022-5193(78)90022-X

79. Tackenberg MC, Hughey JJ. The risks of using the chi-square periodogram to estimate the period of biological rhythms. *PLoS Comput Biol*. 2021;17(1):1-16. doi:10.1371/JOURNAL.PCBI.1008567

80. Chapman JJ, Roberts JA, Nguyen VT, Breakspear M. Quantification of free-living activity patterns using accelerometry in adults with mental illness. *Sci Rep*. 2017;7(March):1-12. doi:10.1038/srep43174

81. Fasmer OB, Hauge E, Berle JØ, Dilsaver S, Oedegaard KJ. Distribution of active and resting periods in the motor activity of patients with depression and schizophrenia. *Psychiatry Investig*. 2016;13(1):112-120. doi:10.4306/pi.2016.13.1.112

82. Edgar N, McClung CA. Major depressive disorder: a loss of circadian synchrony? *Bioessays*. 2013;35(11):940-944. doi:10.1002/bies.201300086

83. Cornelissen G. Cosinor-based rhythmometry. *Theor Biol Med Model*. 2014;11(1):16. doi:10.1186/1742-4682-11-16

84. Austin PC, Steyerberg EW. The number of subjects per variable required in linear regression analyses. *J Clin Epidemiol*. 2015;68(6):627-636. doi:10.1016/j.jclinepi.2014.12.014

85. Duru G, Fantino B. The clinical relevance of changes in the Montgomery-Asberg Depression Rating Scale using the minimum clinically important difference approach. *Curr Med Res Opin*. 2008;24(5):1329-1335. doi:10.1185/030079908X291958

86. Wilcox AG, Bains RS, Williams D, et al. Zfhx3-mediated genetic ablation of the SCN abolishes light entrainable circadian activity while sparing food anticipatory activity. *iScience*. 2021;24(10):103142. doi:10.1016/j.isci.2021.103142

87. Mistlberger RE, Skene DJ. Social influences on mammalian circadian rhythms: Animal and human studies. *Biol Rev Camb Philos Soc*. 2004;79(3):533-556. doi:10.1017/S1464793103006353

88. Sagvolden T, Russell VA, Aase H, Johansen EB, Farshbaf M. Rodent models of attention-deficit/hyperactivity disorder. *Biol Psychiatry*. 2005;57(11):1239-1247. doi:10.1016/j.biopsych.2005.02.002

89. Huang G-J, Herbert J. Stimulation of neurogenesis in the hippocampus of the adult rat by fluoxetine requires rhythmic change in corticosterone. *Biol Psychiatry*. 2006;59(7):619-624. doi:10.1016/j.biopsych.2005.09.016

90. Pariante CM, Makoff A, Lovestone S, et al. Antidepressants enhance glucocorticoid receptor function in vitro by modulating the membrane steroid transporters. *Br J Pharmacol*. 2001;134(6):1335-1343. doi:10.1038/sj.bjp.0704368

91. Pariante CM, Kim RB, Makoff A, Kerwin RW. Antidepressant fluoxetine enhances glucocorticoid receptor function in vitro by modulating membrane steroid transporters. *Br J Pharmacol*. 2003;139(6):1111-1118. doi:10.1038/sj.bjp.0705357

92. Bose R, Spulber S, Kilian P, et al. Tet3 mediates stable glucocorticoid-induced alterations in DNA methylation and Dnmt3a/Dkk1 expression in neural progenitors. *Cell Death Dis*. 2015;6(6):1-8. doi:10.1038/cddis.2015.159

93. Mieda M, Ono D, Hasegawa E, et al. Cellular clocks in AVP neurons of the scn are critical for interneuronal coupling regulating circadian behavior rhythm. *Neuron*. 2015;85(5):1103-1116. doi:10.1016/j.neuron.2015.02.005

94. Yamaguchi Y, Suzuki T, Mizoro Y, et al. Mice Genetically Deficient in Vasopressin V1a and V1b Receptors Are Resistant to Jet Lag. *Science*. 2013;342(6154):85-90. doi:10.1126/science.1238599

95. Kiessling S, Eichele G, Oster H. Adrenal glucocorticoids have a key role in circadian resynchronization in a mouse model of jet lag. *J Clin Invest*. 2010;120(7):2600-2609. doi:10.1172/JCI41192

96. Sage D, Ganem J, Guillaumond F, et al. Influence of the Corticosterone Rhythm on Photic Entrainment of Locomotor Activity in Rats. *J Biol Rhythms*. 2004;19(2):144-156. doi:10.1177/0748730403261894

97. Mohawk JA, Cashen K, Lee TM. Inhibiting cortisol response accelerates recovery from a photic phase shift. *Am J Physiol Regul Integr Comp Physiol*. 2005;288(1):R221-8. doi:10.1152/ajpregu.00272.2004

98. Häggendal J, Hamberger B. Quantitative in Vitro Studies on Noradrenaline Uptake and its Inhibition by Amphetamine, Desipramine and Chlorpromazine. *Acta Physiol Scand*. 1967;70(3-4):277-280. doi:10.1111/j.1748-1716.1967.tb03626.x

99. Vacher CM, Frétier P, Créminon C, et al. Monoaminergic control of vasopressin and VIP expression in the mouse suprachiasmatic nucleus. *J Neurosci Res*. 2003;71(6):791-801. doi:10.1002/jnr.10529

100. Vacher CM, Calas A, Maltonti F, Hardin-Pouzet H. Postnatal regulation by monoamines of vasopressin expression in the neuroendocrine hypothalamus of MAO-A-deficient mice. *Eur J Neurosci.* 2004;19(4):1110-1114. doi:10.1111/j.1460-9568.2004.03201.x

101. Vacher CM, Fretier P, Creminon C, Calas A, Hardin-Pouzet H. Activation by serotonin and noradrenaline of vasopressin and oxytocin expression in the mouse paraventricular and supraoptic nuclei. *J Neurosci.* 2002;22(5):1513-22. doi:22/5/1513 [pii]

102. Funato H, Kobayashi A, Watanabe Y. Differential effects of antidepressants on dexamethasone-induced nuclear translocation and expression of glucocorticoid receptor. *Brain Res.* 2006;7:125-134. doi:10.1016/j.brainres.2006.08.029

103. Lai M, McCormick JA, Chapman KE, Kelly PAT, Seckl JR, Yau JLW. Differential regulation of corticosteroid receptors by monoamine neurotransmitters and antidepressant drugs in primary hippocampal culture. *Neuroscience.* 2003;118(4):975-984. doi:10.1016/S0306-4522(03)00038-1

104. Okugawa G, Omori K, Suzukawa J, Fujiseki Y, Kinoshita T, Inagaki C. Long-term treatment with antidepressants increases glucocorticoid receptor binding and gene expression in cultured rat hippocampal neurones. *J Neuroendocrinol.* 1999;11(11):887-895. doi:10.1046/j.1365-2826.1999.00405.x

105. Rossby SP, Nalepa I, Huang M, et al. Norepinephrine-independent regulation of GRII mRNA in vivo by a tricyclic antidepressant. *Brain Res.* 1995;687(1-2):79-82. doi:10.1016/0006-8993(95)00459-4

106. Bellet MM, Vawter MP, Bunney BG, Bunney WE, Sassone-Corsi P. Ketamine Influences CLOCK:BMAL1 Function Leading to Altered Circadian Gene Expression. Blagosklonny M V., ed. *PLoS One.* 2011;6(8):e23982. doi:10.1371/journal.pone.0023982

107. Bunney BG, Li JZ, Walsh DM, et al. Circadian dysregulation of clock genes: clues to rapid treatments in major depressive disorder. *Mol Psychiatry.* 2014;20(May):1-8. doi:10.1038/mp.2014.138

108. Guardiola-Lemaitre B, De Bodinat C, Delagrange P, Millan MJ, Munoz C, Mocaër E. Agomelatine: mechanism of action and pharmacological profile in relation to antidepressant properties. *Br J Pharmacol.* 2014;171(15):3604-3619. doi:10.1111/bph.12720

109. Regan SL, Williams MT, Vorhees C V. Review of rodent models of attention deficit hyperactivity disorder. *Neurosci Biobehav Rev.* 2022;132:621-637. doi:10.1016/j.neubiorev.2021.11.041

110. Doi M, Yujnovsky I, Hirayama J, et al. Impaired light masking in dopamine D2 receptor–null mice. *Nat Neurosci.* 2006;9(6):732-734. doi:10.1038/nn1711

111. Grippo RM, Güler AD. Dopamine Signaling in Circadian Photoentrainment: Consequences of Desynchrony. *Yale J Biol Med.* 2019;92(2):271-281. http://www.ncbi.nlm.nih.gov/pubmed/31249488.

112. Korshunov KS, Blakemore LJ, Trombley PQ. Dopamine: A Modulator of Circadian Rhythms in the Central Nervous System. *Front Cell Neurosci.* 2017;11. doi:10.3389/fncel.2017.00091

113. Grippo RM, Purohit AM, Zhang Q, Zweifel LS, Güler AD. Direct Midbrain Dopamine Input to the Suprachiasmatic Nucleus Accelerates Circadian Entrainment. *Curr Biol*. 2017;27(16):2465-2475.e3. doi:10.1016/j.cub.2017.06.084

114. Paul JR, Johnson RL, Jope RS, Gamble KL. Disruption of circadian rhythmicity and suprachiasmatic action potential frequency in a mouse model with constitutive activation of glycogen synthase kinase 3. *Neuroscience*. 2012;226:1-9. doi:10.1016/j.neuroscience.2012.08.047

115. Zhang K, Song X, Xu Y, et al. Continuous GSK-3β overexpression in the hippocampal dentate gyrus induces prodepressant-like effects and increases sensitivity to chronic mild stress in mice. *J Affect Disord*. 2013;146(1):45-52. doi:10.1016/j.jad.2012.08.033

116. Rybak YE, McNeely HE, Mackenzie BE, Jain UR, Levitan RD. An Open Trial of Light Therapy in Adult Attention-Deficit/Hyperactivity Disorder. *J Clin Psychiatry*. 2006;67(10):1527-1535. doi:10.4088/JCP.v67n1006

117. Korman M, Palm D, Uzoni A, et al. ADHD 24/7: Circadian clock genes, chronotherapy and sleep/wake cycle insufficiencies in ADHD. *World J Biol Psychiatry*. 2020;21(3):156-171. doi:10.1080/15622975.2018.1523565

118. Rabinowitz J, Schooler NR, Brown B, et al. Consistency checks to improve measurement with the Montgomery-Asberg Depression Rating Scale (MADRS). *J Affect Disord*. 2019;256(December 2018):143-147. doi:10.1016/j.jad.2019.05.077

119. Rabinowitz J, Rabinowitz AA. Outlier-response pattern checks to improve measurement with the Montgomery-Asberg depression rating scale (MADRS). *J Affect Disord*. 2022;299:444-448. doi:10.1016/j.jad.2021.12.076

120. Simmonds-Buckley M, Catarino A, Delgadillo J, Simmonds-Buckley M, Catarino A, Delgadillo J. Depression subtypes and their response to cognitive behavioral therapy: A latent transition analysis. *Depress Anxiety*. 2021;38(9):907-916. doi:10.1002/da.23161

121. Catarino A, Fawcett JM, Ewbank MP, et al. Refining our understanding of depressive states and state transitions in response to cognitive behavioural therapy using latent Markov modelling. *Psychol Med*. 2022;52(2):332-341. doi:10.1017/S0033291720002032

122. Fantino B, Moore N. The self-reported Montgomery-Åsberg depression rating scale is a useful evaluative tool in major depressive disorder. *BMC Psychiatry*. 2009;9(1):26. doi:10.1186/1471-244X-9-26

123. Hermens MLM, Adèr HJ, van Hout HPJ, Terluin B, van Dyck R, de Haan M. Administering the MADRS by telephone or face-to-face: a validity study. *Ann Gen Psychiatry*. 2006;5:3. doi:10.1186/1744-859X-5-3

124. Targum SD, Catania CJ. Audio-digital recordings for surveillance in clinical trials of major depressive disorder. *Contemp Clin Trials Commun*. 2019;14:100317. doi:10.1016/j.conctc.2019.100317

125. Hudgens S, Floden L, Blackowicz M, et al. Meaningful Change in Depression Symptoms Assessed with the Patient Health Questionnaire (PHQ-9) and Montgomery-Åsberg Depression Rating Scale (MADRS) Among Patients with Treatment Resistant Depression in Two, Randomized, Double-blind, Active-controlled Tr. *J Affect Disord*.

2021;281:767-775. doi:10.1016/j.jad.2020.11.066

126. Taliaz D, Spinrad A, Barzilay R, et al. Optimizing prediction of response to antidepressant medications using machine learning and integrated genetic, clinical, and demographic data. *Transl Psychiatry*. 2021;11(1). doi:10.1038/s41398-021-01488-3

127. Li JZ, Bunney BG, Meng F, et al. Circadian patterns of gene expression in the human brain and disruption in major depressive disorder. *Proc Natl Acad Sci U S A*. 2013;110(24):9950-9955. doi:10.1073/pnas.1305814110

128. Helgadóttir B, Forsell Y, Hallgren M, Möller J, Ekblom Ö. Long-term effects of exercise at different intensity levels on depression: A randomized controlled trial. *Prev Med (Baltim)*. 2017;105(July):37-46. doi:10.1016/j.ypmed.2017.08.008

129. Morres ID, Hatzigeorgiadis A, Stathi A, et al. Aerobic exercise for adult patients with major depressive disorder in mental health services: A systematic review and meta-analysis. *Depress Anxiety*. 2019;36(1):39-53. doi:10.1002/da.22842

130. Morres ID, Hatzigeorgiadis A, Krommidas C, et al. Objectively measured physical activity and depressive symptoms in adult outpatients diagnosed with major depression. Clinical perspectives. *Psychiatry Res*. 2019;280:112489. doi:10.1016/j.psychres.2019.112489

131. Mendes-Moreira J, Soares C, Jorge AM, Sousa JF De. Ensemble approaches for regression. *ACM Comput Surv*. 2012;45(1):1-40. doi:10.1145/2379776.2379786

132. Pagani L, Semenova EA, Moriggi E, et al. The Physiological Period Length of the Human Circadian Clock In Vivo Is Directly Proportional to Period in Human Fibroblasts. Reif A, ed. *PLoS One*. 2010;5(10):e13376. doi:10.1371/journal.pone.0013376

133. Hasan S, Santhi N, Lazar AS, et al. Assessment of circadian rhythms in humans: comparison of real-time fibroblast reporter imaging with plasma melatonin. *FASEB J*. 2012;26(6):2414-2423. doi:10.1096/fj.11-201699

134. Brown SA, Kunz D, Dumas A, et al. Molecular insights into human daily behavior. *Proc Natl Acad Sci*. 2008;105(5):1602-1607. doi:10.1073/pnas.0707772105